Check for updates

Global Biogeochemical Cycles

RESEARCH ARTICLE
10.1029/2024GB008209

Agricultural Land Use Impacts Aquatic Greenhouse Gas Emissions From Wetlands in the Canadian Prairie Pothole Region

L. A. Logozzo[1,2], C. Soued[1], L. E. Bortolotti[3], P. Badiou[3], P. Kowal[3], B. Page[3], and M. J. Bogard[1]

[1]Department of Biological Sciences, University of Lethbridge, Lethbridge, AB, Canada, [2]Now at Hudson River Foundation, New York, NY, USA, [3]Institute for Wetland and Waterfowl Research, Ducks Unlimited Canada, Stonewall, MB, Canada

Abstract The Prairie Pothole Region (PPR) is the largest wetland complex in North America, with millions of wetlands punctuating the landscapes of Canada and the United States. Here, wetlands have been dramatically impacted by agricultural land use, with unclear implications for regional to global greenhouse gas (GHG) emissions budgets. By surveying wetlands across all three Canadian prairie provinces in the PPR, we show that emissions patterns of carbon dioxide (CO_2), methane (CH_4), and nitrous oxide (N_2O) from aquatic habitats differ among wetlands embedded in cropland versus perennial landcover. Wetlands in cropped landscapes had double the aquatic diffusive emissions (17.8 ± 29.3 vs. 7.7 ± 13.9 g CO_2-*eq* m^{-2} d^{-1}) largely driven by CH_4. Structural equation modeling showed that all three GHGs responded differently to the surrounding landscape properties. Emissions of CH_4 were the most sensitive to land use, responding positively to the elevated phosphorus content and lower sulfate content in cropped settings, despite higher organic matter content in wetlands in perennial landscapes. Aquatic N_2O emissions were negligible, while CO_2 emissions were high, but not strongly related to agricultural land use. While our estimates of aquatic CH_4 emissions from PPR wetlands were high (15.6 ± 37.2 mmol CH_4 m^{-2} d^{-1}), accounting for fluxes from vegetated and soil habitats would lead to whole-wetland emissions rates that are lower and comparable to wetlands in other biomes. Our study represents an important step toward understanding wetland emission responses to land use in the PPR and other wetland-rich agricultural landscapes.

Plain Language Summary Wetlands are potentially important natural climate solutions as they uptake carbon dioxide and store carbon in plants and soils. Therefore, wetland protection or restoration in regions with a high density of wetlands such as the Canadian Prairies could help Canada meet its climate goals. Wetlands also emit greenhouse gases (GHGs) such as carbon dioxide, methane, and nitrous oxide, which reduce their net capacity to sequester carbon. Moreover, agricultural practices such as cropping and livestock grazing, common in the Canadian Prairies and most global regions, impact nearby wetlands, but the effects on wetland GHG emissions are unclear. We studied wetlands in all three Canadian Prairie provinces to determine whether surrounding agricultural land use shaped wetland water characteristics and GHG emissions. We found that wetlands located in fields with crops had higher nutrient content (phosphorous) and lower salt content (sulfate), which increased methane emissions compared to wetlands in grazed and idled grasslands. Higher methane emissions from wetlands in cropland doubled the total GHG emissions in carbon dioxide equivalents compared with wetlands in grassland. This study informs how agricultural management practices can reduce wetland GHG emissions and provides estimates of wetland GHG emissions for one of the largest wetland complexes in the world.

Key Points:

- Wetlands in cropland had higher phosphorous and lower sulfate concentrations than those in perennially vegetated landscapes
- Phosphorous and sulfate content predicted aquatic methane but not carbon dioxide or nitrous oxide concentrations
- Wetlands in cropland had greater aquatic diffusive methane emissions versus perennial landcover, doubling the total diffusive greenhouse gas flux

Supporting Information:

Supporting Information may be found in the online version of this article.

Correspondence to:

L. A. Logozzo,
laura@hudsonriver.org

Citation:

Logozzo, L. A., Soued, C., Bortolotti, L. E., Badiou, P., Kowal, P., Page, B., & Bogard, M. J. (2025). Agricultural land use impacts aquatic greenhouse gas emissions from Wetlands in the Canadian Prairie Pothole Region. *Global Biogeochemical Cycles*, *39*, e2024GB008209. https://doi.org/10.1029/2024GB008209

Received 22 APR 2024
Accepted 20 JAN 2025
Corrected 2 MAY 2025

This article was corrected on 2 MAY 2025. See the end of the full text for details.

Author Contributions:

Conceptualization: C. Soued, L. E. Bortolotti, P. Badiou, M. J. Bogard
Data curation: L. A. Logozzo, C. Soued, P. Kowal, B. Page
Formal analysis: L. A. Logozzo, C. Soued
Funding acquisition: L. E. Bortolotti, P. Badiou, M. J. Bogard
Investigation: L. A. Logozzo, L. E. Bortolotti, M. J. Bogard

© 2025 The Author(s).
This is an open access article under the terms of the Creative Commons Attribution-NonCommercial License, which permits use, distribution and reproduction in any medium, provided the original work is properly cited and is not used for commercial purposes.

1. Introduction

Wetlands are highly productive ecosystems that sequester large quantities of carbon (C) relative to their small areal footprint (Mitsch et al., 2013). Globally, around 3.4 million km^2 of inland wetlands have been lost to human land use conversion since 1700 (Fluet-Chouinard et al., 2023). Because of this, wetland conservation (minimizing further losses) and restoration have been proposed as nature-based climate solutions (Drever et al., 2021; Griscom et al., 2017). Wetlands also naturally emit greenhouse gases (GHGs) such as carbon dioxide (CO_2), methane (CH_4), and nitrous oxide (N_2O). Elevated GHG emissions—particularly CH_4—can reduce net C sequestration potential and limit the role that wetlands can play in a nature-based climate solutions context (Badiou et al., 2011),

19449224, 2025, 3, Downloaded from https://agupubs.onlinelibrary.wiley.com/doi/10.1029/2024GB008209 by University Of Lethbridge, Wiley Online Library on [09/07/2025]. See the Terms and Conditions (https://onlinelibrary.wiley.com/terms-and-conditions) on Wiley Online Library for rules of use; OA articles are governed by the applicable Creative Commons License

Methodology: L. A. Logozzo, C. Soued, L. E. Bortolotti, P. Badiou, P. Kowal, B. Page, M. J. Bogard
Project administration: L. E. Bortolotti, P. Badiou, P. Kowal, B. Page, M. J. Bogard
Resources: L. A. Logozzo, C. Soued, L. E. Bortolotti, P. Badiou, P. Kowal, B. Page, M. J. Bogard
Software: C. Soued
Supervision: L. E. Bortolotti, P. Badiou, M. J. Bogard
Validation: L. A. Logozzo, C. Soued, P. Kowal, M. J. Bogard
Visualization: L. A. Logozzo
Writing – original draft: L. A. Logozzo, M. J. Bogard
Writing – review & editing: L. A. Logozzo, C. Soued, L. E. Bortolotti, P. Badiou, P. Kowal, B. Page, M. J. Bogard

at least over shorter decadal timescales (Neubauer & Megonigal, 2015). Scaled globally, wetland GHG emissions are significant; Rosentreter et al. (2021) found that freshwater wetlands emit an average of 150 Tg CH_4 y^{-1}, which is greater than 30% of CH_4 emissions from all other aquatic ecosystems combined. Although GHG emissions are generally accounted for when estimating wetland C storage budgets (Badiou et al., 2011; Drever et al., 2021; Mitsch et al., 2013), there are still significant uncertainties in wetland GHG flux estimates (Rosentreter et al., 2021), particularly when accounting for the effects of anthropogenic impacts, like agricultural land use, on current and future rates of emissions (Gauci et al., 2004; Petrescu et al., 2015).

The Prairie Pothole Region (PPR) has the largest concentration of inland wetlands in North America (Euliss et al., 2006). It consists predominantly of isolated depressional mineral wetlands that formed during deglaciation. The Canadian PPR, spanning the Canadian provinces of Alberta, Saskatchewan, and Manitoba, is also an important region for food production, where it is estimated that between 40% and 70% of wetlands have been lost since European colonization (Conly & van der Kamp, 2001; Environment Canada, 1986; Muhammad et al., 2018), predominantly due to agricultural and urbanization practices such as wetland drainage. Restored wetlands in this region have been shown to store more C than they emit (Badiou et al., 2011), and the rate of C emissions tends to decrease with time since restoration (Bortolotti et al., 2016). Recent analysis demonstrated that in Canada, the climate mitigation potential via wetland preservation and avoided emissions (3.1 Tg CO_2-*eq* y^{-1}) is almost 8 times greater than that of restoring wetlands, though the combined potential of protection and restoration may be larger (Drever et al., 2021). Thus, wetland restoration and conservation in the PPR may be a viable natural climate solution, which can help Canada meet its C emissions reductions goal of 40%–45% of 2005 levels by 2030 (Environment and Climate Change Canada, 2022).

Numerous, sometimes opposing factors drive the production, transport, consumption, and fluxes of CO_2, CH_4, and N_2O, making the prediction of net radiative forcing from wetland habitats in the PPR challenging. In inland waters, CO_2 is predominantly produced from the photo- or bio-mineralization of organic carbon (OC) and from some forms of chemical weathering, while CO_2 is consumed during photosynthesis (Tranvik et al., 2009). Ambient temperature impacts the rates of microbial OC mineralization (Apple et al., 2006; Gudasz et al., 2010) and the solubility of CO_2. In shallow wetland systems, CH_4 production is predominantly driven by methanogenesis, the least thermodynamically favorable oxidation-reduction (redox) microbial C decomposition process, which mainly occurs in anoxic soils and sediment (Krüger et al., 2001). CH_4 can be oxidized to CO_2 under aerobic conditions and anaerobic CH_4 oxidation may also occur with the reduction of other redox-sensitive species such as sulfate (SO_4^{2-}), nitrate (NO_3^-), and ferric iron (Fe^{3+}) (Martinez-Cruz et al., 2018; Segarra et al., 2015). Thus, CH_4 concentrations in wetlands are dependent on the concentrations of other more thermodynamically favorable terminal electron acceptors (TEAs; e.g., oxygen, NO_3^-, SO_4^{2-}) (Burgin et al., 2011; Krüger et al., 2001), OC bio-lability and amount (Dalcin Martins et al., 2017; Soued et al., 2024), and temperature (Yvon-Durocher et al., 2014). Relevant to CH_4 cycling, sulfate (SO_4^{2-}) concentrations in PPR wetlands tend to be high, on average, due to groundwater chemical weathering processes and the geology of the region (Goldhaber et al., 2014). Consequently, CH_4 emissions can be low despite elevated trophic status (Soued et al., 2024). Microbial nitrification and denitrification are the predominant biotic processes producing N_2O under aerobic and anaerobic conditions, respectively. Nitrate (NO_3^-) concentration, OC bio-lability, redox conditions, temperature, and pH can all impact N_2O production (Burgin & Hamilton, 2007; Speir et al., 2023). Denitrification can also consume N_2O, and thus simultaneous production and consumption can occur under the same conditions (Webb, Hayes, et al., 2019). All these mechanisms can occur in tandem, counteracting one another or acting synergistically, ultimately complicating the prediction of GHG emissions rates at both wetland and broader scales.

Despite the complexity of GHG mechanistic drivers, previous empirical surveys have found that CH_4 emissions are most strongly predicted by chlorophyll *a* concentrations (Beaulieu et al., 2019; DelSontro et al., 2018), nutrient content (Jensen et al., 2023; Webb, Leavitt, et al., 2019), and wetland size (Bansal et al., 2023). The rate of emissions of both CO_2 and N_2O are typically less well explained in empirical models; however, CO_2 is best predicted by internal metabolism (Jensen et al., 2023; Webb, Leavitt, et al., 2019), groundwater alkalinity (Webb, Leavitt, et al., 2019), and nutrient concentrations (DelSontro et al., 2016), while N_2O is best predicted by stratification (agricultural reservoirs), nitrogen loading (Tangen & Bansal, 2022; Webb, Hayes, et al., 2019), and chlorophyll *a* (DelSontro et al., 2018). Although CH_4 emissions seem to be the most important contributor to the total GHG flux on a 100-year time scale (in CO_2 equivalents) (Beaulieu et al., 2019; Jensen et al., 2023; Webb, Leavitt, et al., 2019), it is unknown whether this would change with land use, and most empirical surveys do not measure all three GHGs in tandem.

19449224, 2025, 3, Downloaded from https://agupubs.onlinelibrary.wiley.com/doi/10.1029/2024GB008209 by University Of Lethbridge, Wiley Online Library on [09/07/2025]. See the Terms and Conditions (https://onlinelibrary.wiley.com/terms-and-conditions) on Wiley Online Library for rules of use; OA articles are governed by the applicable Creative Commons License

It is unclear how anthropogenic disturbances such as agriculture affect GHG cycling and the C storage potential of restored and intact wetland habitats, which is relevant for the Canadian PPR. Conversion of wetland catchments from perennial vegetation landcover to cropland can change the chemical, physical, and biological properties of catchment soils and can further alter wetland water chemistry through nutrient loading and hydrologic shifts (van der Kamp et al., 1999). In cropped landscapes versus perennially vegetated landscapes, wetlands have been shown to emit less CH_4, potentially due to lower soil OC content in croplands (Bansal et al., 2023), whereas other agricultural waterbodies like lakes and reservoirs generally had higher CH_4 emissions (Webb, Leavitt, et al., 2019, but see Chan et al., 2024). Increased aquatic primary productivity under eutrophic conditions may provide more labile OC for CH_4 production (Vachon et al., 2020). At the same time, eutrophication reduces CO_2 emissions in lakes, as higher productivity was associated with greater rates of CO_2 uptake (Balmer & Downing, 2011; DelSontro et al., 2018). N_2O is rarely measured in wetland GHG flux surveys (Badiou et al., 2011; Pennock et al., 2010; Tangen & Bansal, 2022), and so the effects of agriculture on wetland N_2O cycling are poorly constrained (Webb et al., 2021). In cases where N_2O is measured, no clear controls emerge at the regional scale (Soued et al., 2016; Webb, Hayes, et al., 2019), despite strong links between N_2O fluxes and N pollution in other aquatic systems such as rivers (Beaulieu et al., 2011). However, N_2O undersaturation in agricultural reservoirs is common even with high N loading (Webb, Hayes, et al., 2019). This, plus the fact that most N_2O emissions derive from non-inundated wetland habitats (Tangen & Bansal, 2022), suggests that the role of N_2O is likely minor in the emissions budgets of PPR wetland ponds. In summary, mechanisms driving wetland GHG cycling at the regional scale are uncertain in the PPR.

To estimate and predict GHG fluxes from PPR wetlands at a broader regional scale, we require a systematic evaluation of emissions of all three GHGs from wetlands under distinct land uses. Here, we explore the effects of two distinct agricultural land uses (cropping versus perennial vegetation for livestock grazing) on the aquatic emissions of CO_2, CH_4, and N_2O from PPR wetlands. Our goal is to compare emissions from the two land use categories and identify potential mechanisms behind these patterns. This can be used to inform agricultural management decisions to optimize C storage and reduce wetland GHG emissions in agricultural landscapes.

2. Materials and Methods

2.1. Site Descriptions

Sites were located in the Canadian PPR, an approximately 498,000 km^2 region (U.S. Geological Survey, 2015). Wetlands were sampled across the three Canadian PPR provinces (Alberta, Saskatchewan, and Manitoba). The number of wetlands sampled in cropped versus grazed or idled perennially vegetated landscapes was approximately equal for each province (Figure 1, Table S1 in Supporting Information S1; n = 7–8 and 8, respectively). A total of 22 sites were present in cropped fields and 24 in perennially vegetated cover, which included pasture, idled grassland, and mixed trees (Table S1 in Supporting Information S1). Overall, 471 samples (and corresponding ambient air for each sample) were collected throughout May–October 2021. Most wetlands were sampled approximately monthly, though 15 sites were sampled less than once a month due to drying in summer (Table S1 in Supporting Information S1). The distribution of samples from cropland and perennially vegetated sites was approximately equal over the sampling period (n = 236 and 235, respectively). To better constrain within-wetland spatial variation in aquatic GHG content, a subset of sites were repeatedly sampled at multiple open-water stations (typically n = 4) (Table S1 in Supporting Information S1).

2.2. Water Quality Parameters

At each site, water temperature was measured using a YSI EXO1 multiparameter probe in Alberta sites and with a thermometer in the Saskatchewan and Manitoba sites. Water samples were collected from three locations within each wetland site, 10–20 cm below the water surface, and then consolidated into a triple rinsed container. The sample was split into three fractions that were stored on ice and shipped in coolers. One set of samples were measured for pH and SO_4^{2-} concentrations by ion chromatography (EPA 300.1 mod) by ALS laboratories in Winnipeg, Canada. Of the remaining water, a portion was filtered upon collection using glass fiber filters (GF/C, nominal pore size 1.2 μm) for dissolved nutrient analysis, and the remaining unfiltered fraction was transferred to a container for total nutrient analysis. These samples were shipped to the Agriculture and Agri-Food Canada's Brandon Research and Development Center in Manitoba, Canada, and then frozen prior to analysis. A flow analyzer was used to measure unfiltered NH_4^+ and NO_x (as $NO_3^- + NO_2^-$) concentrations colorimetrically. Total

19449224, 2025, 3, Downloaded from https://agupubs.onlinelibrary.wiley.com/doi/10.1029/2024GB008209 by University Of Lethbridge, Wiley Online Library on [09/07/2025]. See the Terms and Conditions (https://onlinelibrary.wiley.com/terms-and-conditions) on Wiley Online Library for rules of use; OA articles are governed by the applicable Creative Commons License

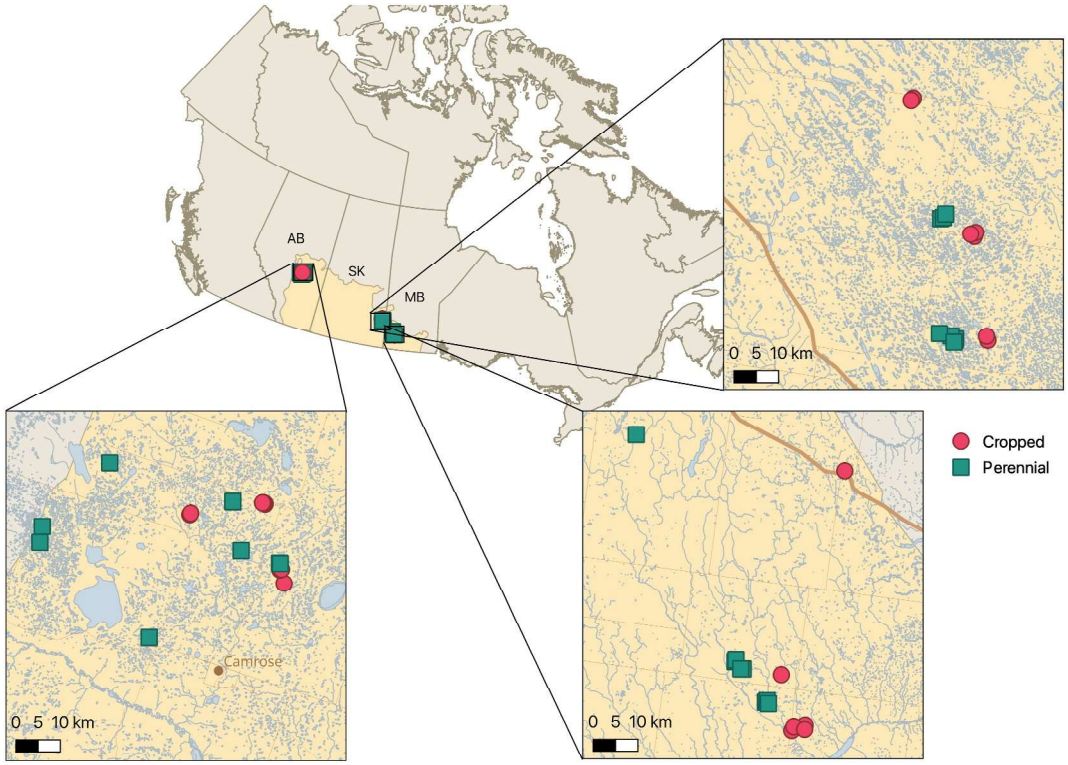

Figure 1. Wetland sites (points) were sampled monthly from May to October in 2021. Yellow area indicates the Canadian Prairie Pothole Region (U.S. Geological Survey, 2015). Wetland sites are designated by their upland land use: cropland or perennially vegetated land cover.

dissolved N (TDN) and dissolved organic carbon (DOC) concentrations were determined through the combustion method using a Shimadzu TOC-VCSn analyzer. Total P and total dissolved P (TDP) concentrations were determined through sulfuric acid/persulfate digestions and colorimetrically using the ascorbic acid method.

2.3. GHG Sampling and Analysis

For GHG analysis, 105 mL of water was collected in the open water portion of each wetland roughly 25 cm below the air-water interface in an airtight 140 mL plastic syringe. A 35 mL headspace was created with ambient air on site with the air to water ratio = 0.33. To equilibrate the gas and water phases, the closed container was shaken for at least 3 min. As much of the 35 mL gas phase as possible (typically at least 25 mL) was then transferred to a pre-evacuated 12 mL exetainer (Labco) with an airtight butyl rubber stopper. The water temperature in the syringe was then measured using a handheld thermometer. Ambient air samples were also collected on site at all wetlands (one vial per site). The over pressurized vials were stored in the dark at room temperature until later analysis in the laboratory. The partial pressure of GHGs in each vial was measured using a Thermo Trace 1310 gas chromatograph. A detailed description of the instrument setup, analysis, and calibration is provided in Chan et al. (2024). A methanizer-equipped flame ionization detector was used to measure CO_2 and CH_4 content in the samples. An electron capture detector was used to measure N_2O content. To estimate the partial pressure of each gas from the curve area, either linear or polynomial calibration curves were generated with standards of CO_2, CH_4, and N_2O (199–39,950, 0.9–508, and 0.15–198.5 ppm, respectively). When CH_4 concentrations were beyond the linear range of the calibration curve, samples were rerun after diluting with pure N_2.

2.4. GHG Partial Pressure and Diffusive Emissions Calculations

For each sample, the in situ partial pressure and dissolved concentrations of each GHG were back-calculated based on the gas solubility (dependent on salinity and water temperature) before and after equilibration, local atmospheric pressure, and the headspace air to water ratio. Areal GHG emissions rates were calculated as

$$fCO_2, fCH_4, fN_2O = k_{gas} * (C_{gas} - C_{equilib}) \quad (1)$$

where C_{gas} and $C_{equilib}$ represent the measured gas concentration in water and concentration of gas in equilibrium with the atmosphere, respectively, and k_{gas} represents the specific gas transfer velocity of each GHG. To calculate k_{gas}, we followed Soued and Prairie (2020). Specifically, we used the following equation from Cole and Caraco (1998):

$$k_{gas} = k_{600}\left(\frac{Sc_{gas}}{Sc_{600}}\right)^{n} \quad (2)$$

where k_{600} is the mean gas transfer velocity standardized to a Schmidt number (Sc_{600}) of 600 at 20°C, Sc_{gas} is the gas-specific Schmidt number calculated from empirical equations (Wanninkhof, 1992) for a specific water temperature and density, and n is a constant that we made equal to 0.67 (but which can vary from −0.67 to −0.5; Jähne et al., 1987; Ledwell, 1984). We calculated k_{600} (Figure S1a in Supporting Information S1) using an empirical equation from Klaus and Vachon (2020) that estimates gas transfer velocity using daily average wind speed and the open water surface area (fetch) of an ecosystem:

$$k_{600} = \left(a \cdot \log_{10} A + aj\right) \cdot U + c \cdot \text{logit}\, SIN + cj \quad (3)$$

Where A is the open water area (km^2), U is wind speed ($m\ s^{-1}$) and SIN is space integration (method-related footprint area divided by area), which was made equal to 0.999. The coefficients a, aj, c, and cj were modeled using a mixed-effects model and by picking new parameter values by sampling from multivariate normal distribution based on fit. We used the average hourly wind speed recorded for the 24 hr preceding sampling and atmospheric pressure recorded at the nearest federal or provincial weather station (Figure S1b in Supporting Information S1). The station numbers used here include Brandon A (Climate ID 5010481), Shoal Lake CS (5012654), Roblin (5012469), Yorkton (4019075), Camrose (3011240), and Wetaskiwin AGCM (3017282). The surface area of each wetland was obtained by manual delineation of open water from 2021 Google Earth imagery.

2.5. Historical Land Suitability for Agriculture

In order to establish potential preexisting soil differences across the land use categories, we used the Canada Land Inventory (CLI) (Agriculture and Agri-Food Canada, 1998) to determine differences in historical (1971–1994) soil properties between sites. These data categorize soil by agricultural capability and limitation at a 1:250,000 scale (approximate resolution of 25 m). Each polygon in the CLI is designated 1–3 CLI classes and subclasses with the proportion of the total polygon area that is in each class and subclass. Sampling sites were classified by their agricultural land suitability class(es) (Table S2 in Supporting Information S1) and subclass(es) (Table S3 in Supporting Information S1) in QGIS v. 3.28.15 (QGIS Development Team, 2020) by joining CLI classification polygons and wetland site attributes based on location. The predominant (>50% of polygon area) class and subclass for each site are presented in Table S1 in Supporting Information S1. CLI class values (1–7) increased by degree of limitation, with lower class numbers being more suitable for crops, up to 7, which is non-arable land. The specific agricultural limitations are described by subclass in Table S3 in Supporting Information S1.

2.6. Statistical Analyses

All statistical analyses were performed in R v. 4.2.2 (R Core Team, 2022). Mean or median values were presented with the standard deviation (S.D.), denoted as mean or median ± S.D. Greenhouse gas partial pressures were presented on a $\log_{10}$ scale. There were 17 observations of negative values for pCO_2, likely due to a lack of alkalinity correction on estimates of pCO_2. These 17 negative values were removed from the data set. For the fluxes (fCO_2, fCH_4, and fN_2O), a pseudo log-scale (Wickham et al., 2023) that transitions from a log-scale to a linear-scale near zero (Figure S2 in Supporting Information S1) was used to plot negative flux values. This transformation allows for the plotting and statistical analysis of negative fluxes, which have biogeochemical significance. Data distributions appeared closer to normal following the transformation (Figure S3 in Supporting Information S1). More details on the pseudo-log transformations applied to flux data are provided in Text S1 in Supporting Information S1.

19449224, 2025, 3, Downloaded from https://agupubs.onlinelibrary.wiley.com/doi/10.1029/2024GB008209 by University Of Lethbridge, Wiley Online Library on [09/07/2025]. See the Terms and Conditions (https://onlinelibrary.wiley.com/terms-and-conditions) on Wiley Online Library for rules of use; OA articles are governed by the applicable Creative Commons License

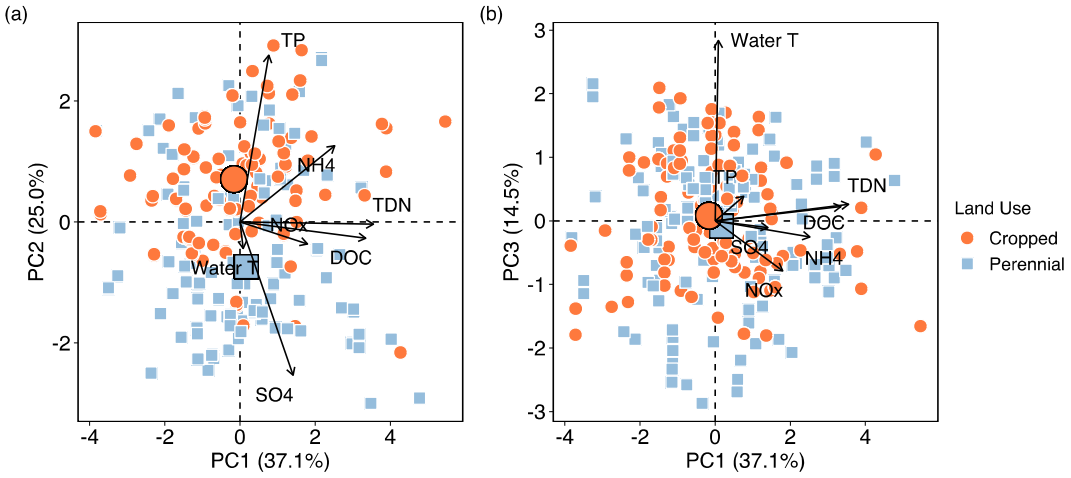

Figure 2. Biplot of the scores (points) and loadings (arrows) from the principal component analysis (PCA) of water chemistry parameters. The axes are PC1 and PC2 (a) and PC1 and PC3 (b). Scores are color coded by land use (wetlands in cropped vs. perennially vegetated landscapes), and the two larger points outlined in black represent the mean scores for each land use category.

Differences across categories (e.g., land use) were evaluated on transformed data by one-way or two-way ANOVAs using the aov() function in the *stats* package (R Core Team, 2022). Following ANOVA, we used quantile-quantile plots (qqPlot() in the *car* package) to test the normality of the residuals, and we plotted residuals versus the fitted values to test the homogeneity of variances. When the distribution of residuals of the one-way ANOVA did not meet normality assumptions, one-way comparisons across categories were instead evaluated using a Kruskal-Wallis test (kruskal.wallis() function in *stats*) on untransformed data. ANOVA or Kruskal-Wallis *p*-values were presented when discussing whether observed differences across categories were significant. Relationships between variables were determined using linear regressions (lm() function in *stats*), from which R-squared (R^2) values and *p*-values were presented. For non-significant relationships ($p > 0.05$), trendlines and R^2 values were not presented.

We used principal component analysis (PCA) to summarize wetland water chemistry and to evaluate water chemistry drivers of GHG emissions. PCA was performed using the following $\log_{10}$ transformed variables: total phosphorous (TP), total dissolved nitrogen (TDN), nitrate and nitrite (NO_x), ammonium (NH_4^+), sulfate (SO_4^{2-}), and dissolved organic carbon (DOC). Water temperature (untransformed) was also included in the PCA. All variables were scaled by mean-centering and dividing by the standard deviation using the scale() function. PCA was performed using the princomp() function from *stats*. Two to three principal components were determined to be significant by comparison to the Allen (Allen & Hubbard, 1986) and Longman (Longman et al., 1989) thresholds using parallel analysis (Figure S4 in Supporting Information S1). Regional GHG drivers were further explained using a structural equation model (SEM) performed using the *lavaan* package in R (Yves, 2012). We used scores from principal components 1–3 in the SEM to summarize collinear variables of interest (e.g., TP, SO_4^{2-}). We also included the ordinal historical land use class (Table S2, Figure S5a in Supporting Information S1), the land use category (cropped vs. perennial), the three GHG partial pressures ($\log_{10}$ transformed), and the total GHG flux in the SEM.

3. Results

3.1. Summary of Water Chemistry

Mean values of water chemistry parameters are summarized in Table S4 in Supporting Information S1. The PCA explained 76.6% of the total variance in the data set with three components (Figure S4 in Supporting Information S1). Principal component 1 (PC1, 37.1% of variance explained) was predominantly associated with DOC, TDN, and NH_4^+ (Figures 2a and 2b). Principal component 2 (PC2, 25.0%) was predominantly associated with TP and SO_4^{2-} (Figure 2a). Principal component 3 (PC3, 14.5%) was predominantly associated with water temperature (Figure 2b).

19449224, 2025, 3, Downloaded from https://agupubs.onlinelibrary.wiley.com/doi/10.1029/2024GB008209 by University Of Lethbridge, Wiley Online Library on [09/07/2025]. See the Terms and Conditions (https://onlinelibrary.wiley.com/terms-and-conditions) on Wiley Online Library for rules of use; OA articles are governed by the applicable Creative Commons License

10.1029/2024GB008209

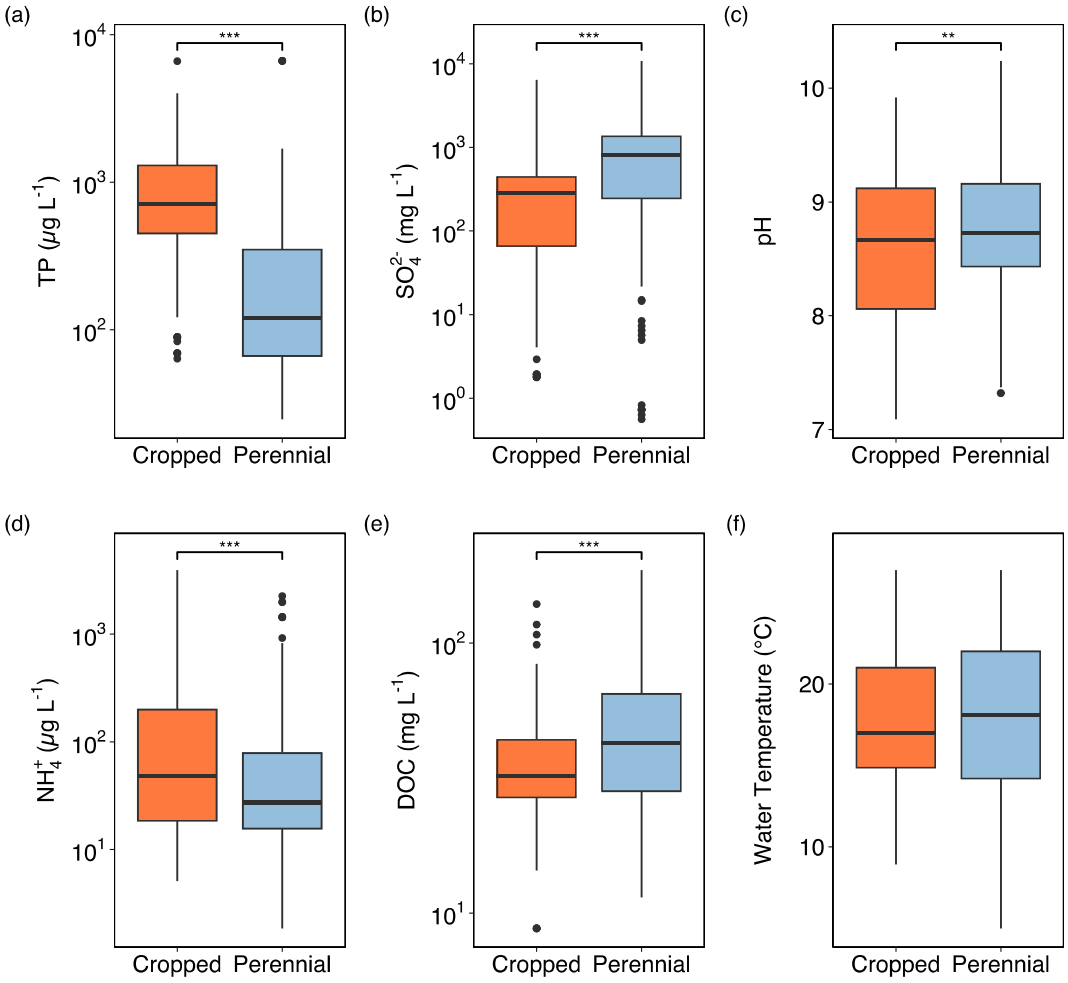

Figure 3. Distribution of wetland water chemistry variables across agricultural land use categories using box plots. The horizontal line in each box represents the median value, the upper and lower ends of each box represent the first and third quartiles, respectively, and the whiskers represent the minimum and maximum values of the data set, excluding outliers. Outliers are plotted as black points. For post hoc comparisons, *, **, and *** denote $p < 0.05$, 0.01, and 0.001, respectively. *y*-axes are on a $\log_{10}$ scale for TP (a), SO_4^{2-} (b), NH_4^+ (d), and DOC (e).

There were significant differences in water chemistry across land use categories. Wetlands in cropped landscapes had significantly higher TP, lower SO_4^{2-}, higher NH_4^+, and lower DOC concentrations than those in perennial cover landscapes ($p < 0.001$, Figure 3). Wetlands in cropped settings also had significantly lower pH than those in perennial settings (Figure 3c, $p = 0.009$). There was no significant difference in water temperature between the land use categories (Figure 3f, $p = 0.89$). Land use impacts were most clearly separated across PC2 (Figure 2a). Specifically, wetlands in cropland had a more positive mean PC2 score than in perennial landscapes, characterized by higher TP and lower SO_4^{2-} (Figure 2a). Although DOC concentrations were on average 26% lower in the cropped wetlands compared to perennial wetlands (Figure 3e), DOC concentrations in cropped wetlands were still high (mean of 37.1 ± 17.3 mg L^{-1}).

Differences in water chemistry across agricultural land use (Figure 3, one-way ANOVA) remained even when accounting for historical differences in soil suitability using a two-way ANOVA (Figure S6 in Supporting Information S1). Some of the wetlands in perennial landscapes were located on less agriculturally suitable soils (Class 5, Figure S5a in Supporting Information S1) compared to cropped landscapes, due to excess water (Subclass W, Figure S5b in Supporting Information S1). However, there was no significant difference in the distribution of soil suitability class or subclass across land use (chi-square test: $p = 0.31$ and 0.45, respectively). Furthermore, differences in water chemistry across land use (Figures 2 and 3 and one-way ANOVA) were still significant even when accounting for historical soil suitability (Figure S6 in Supporting Information S1; two-way

19449224, 2025, 3, Downloaded from https://agupubs.onlinelibrary.wiley.com/doi/10.1029/2024GB008209 by University Of Lethbridge, Wiley Online Library on [09/07/2025]. See the Terms and Conditions (https://onlinelibrary.wiley.com/terms-and-conditions) on Wiley Online Library for rules of use; OA articles are governed by the applicable Creative Commons License

19449224, 2025, 3, Downloaded from https://agupubs.onlinelibrary.wiley.com/doi/10.1029/2024GB008209 by University Of Lethbridge, Wiley Online Library on [09/07/2025]. See the Terms and Conditions (https://onlinelibrary.wiley.com/terms-and-conditions) on Wiley Online Library for rules of use; OA articles are governed by the applicable Creative Commons License

Type III ANOVA with either CLI class or subclass: $p < 0.001$ for TP, SO_4^{2-}, NH_4^+; $p = 0.014$ for DOC with class and $p < 0.001$ for DOC with subclass).

3.2. Summary of Greenhouse Gas Partial Pressures and Fluxes

In terms of partial pressure and flux, the most abundant GHG was CO_2, then CH_4, and then N_2O. Over the sampling period, pCO_2, pCH_4, and pN_2O means were 3901.6 ± 4323.5, 626.9 ± 1550.7, and 0.5 ± 0.8 ppm, respectively (Table S4 in Supporting Information S1). The mean fluxes of CO_2, CH_4, and N_2O were 97.3 ± 125.3, 15.6 ± 37.2, and 0.003 ± 0.016 mmol m^{-2} d^{-1}, respectively (Table S4 in Supporting Information S1). Thus, the mean N_2O flux was essentially zero, and the CO_2 flux was approximately 6 times the CH_4 flux.

The within-site (temporal) variation in the partial pressures and fluxes was lower than the across-site (spatial) variation. For each wetland, the within-site range mean ± standard deviation (SD) of GHG partial pressures was 6745.6 ± 5743.6 for CO_2, 1697.4 ± 3188.2 for CH_4, and 0.9 ± 2.1 ppm for N_2O, compared to the across-site range mean ± SD of 12,358.2 ± 5643.6 for CO_2, 6603.6 ± 7433.7 for CH_4, and 2.9 ± 4.9 ppm for N_2O, respectively. This was equivalent to 1.8, 3.9, and 3.2 times higher across-site (spatial) than within-site (temporal) variation for CO_2, CH_4, and N_2O, respectively. Similarly, the across-site variability in the fluxes were 2.1 and 4.2 times higher than within-site variability for CO_2 and CH_4; the mean range in the across-site GHG fluxes was 399.1 ± 231.0 for CO_2, 170.9 ± 181.7 for CH_4, and 0.100 + 0.104 mmol m^{-2} d^{-1} for N_2O, versus within-site flux ranges of 189.3 ± 153.9 for CO_2, 40.6 ± 72.7 for CH_4, and 0.018 ± 0.039 mmol m^{-2} d^{-1} for N_2O.

3.3. Differences Across Agricultural Land Use

There were significant differences in both the CH_4 partial pressure and flux across land use categories. There was no significant difference in pCO_2 or pN_2O between wetlands in cropped versus perennial landscapes (Kruskal-Wallis test: $p = 0.052$ and 0.060, respectively, Figures 4a and 4c). pCH_4, on the other hand, was significantly higher in wetlands within cropland (931.4 ± 1937.5 ppm) than perennial grassland fields (319.7 ± 930.3 ppm; ANOVA on $\log_{10}pCH_4$: $p < 0.001$, Figure 4b, Table S4 in Supporting Information S1). While there was only a marginal difference in the flux of CO_2 and N_2O between the two land use categories (Kruskal-Wallis test: $p = 0.038$ and 0.070, respectively, Figures 4d and 4f), there was a significantly higher CH_4 flux in wetlands within croplands than perennially vegetated landscapes (Kruskal-Wallis test, $p < 0.001$, Figure 4e). Additionally, the N_2O flux was low regardless of land use (Table S4 in Supporting Information S1). The CH_4 flux had a mean of 23.4 ± 46.6 mmol m^{-2} d^{-1} in the cropped wetlands versus 7.7 ± 21.8 mmol m^{-2} d^{-1} in wetlands in perennially vegetated land (Table S4 in Supporting Information S1). Finally, the total instantaneous GHG flux, in CO_2 equivalents on a 100-year time scale, was also significantly (Kruskal-Wallis test: $p < 0.001$) greater in wetlands in cropped fields than in perennially vegetated fields, predominantly due to the higher CH_4 flux (Figure 5). In fact, the total flux was about double in the wetlands in cropland than in perennial vegetation (1.7 times for the median, and 2.2 times for the mean) (Figure 5, Table S4 in Supporting Information S1).

3.4. Predictors of GHG Flux

Given that land use generally separated out across gradients in PC2 (+TP, $-SO_4$, Figures 2 and 3a), we explored the relationships between these variables and each GHG across land use types. We found an extremely weak, but significant, correlation between $\log_{10}pCO_2$ and PC2 ($R^2 = 0.03$ $p < 0.001$) and no relationship between $\log_{10}pN_2O$ and PC2 ($p = 0.15$). The relationship between $\log_{10}pCH_4$ and PC2, however, was stronger ($R^2 = 0.33$, $p < 0.001$). We also found only a weak, but significant, correlation between $\log_{10}pCO_2$ and $\log_{10}$TP ($R^2 = 0.02$, $p = 0.003$, Figure 6a) and no correlation between $\log_{10}pCO_2$ and $\log_{10}SO_4^{2-}$ ($p = 0.243$, Figure 6b). Similarly, there was no correlation between $\log_{10}pN_2O$ and either $\log_{10}$TP or $\log_{10}SO_4^{2-}$ ($p > 0.1$ for both, Figures 6e and 6f). There was a significant positive correlation between $\log_{10}pCH_4$ and $\log_{10}$TP ($R^2 = 0.28$, $p < 0.001$, Figure 6c) and a significant negative correlation between $\log_{10}pCH_4$ and $\log_{10}SO_4$ ($R^2 = 0.22$, $p < 0.001$, Figure 6d).

We used SEM to evaluate the controls on the total instantaneous GHG flux in CO_2 equivalents. The SEM was significant ($p < 0.001$) and showed that land use had a strong effect on wetland aquatic GHG emissions, largely through water chemistry differences that enhanced CH_4 content in wetlands within cropped landscapes. Land use category (cropland compared to perennial vegetation) had no significant effect ($p = 0.44$) on PC1, which was poorly predicted by both land use and historical soil suitability ($R^2 = 0.06$, Figure 7). On the other hand, PC2 was

19449224, 2025, 3, Downloaded from https://agupubs.onlinelibrary.wiley.com/doi/10.1029/2024GB008209 by University Of Lethbridge, Wiley Online Library on [09/07/2025]. See the Terms and Conditions (https://onlinelibrary.wiley.com/terms-and-conditions) on Wiley Online Library for rules of use; OA articles are governed by the applicable Creative Commons License

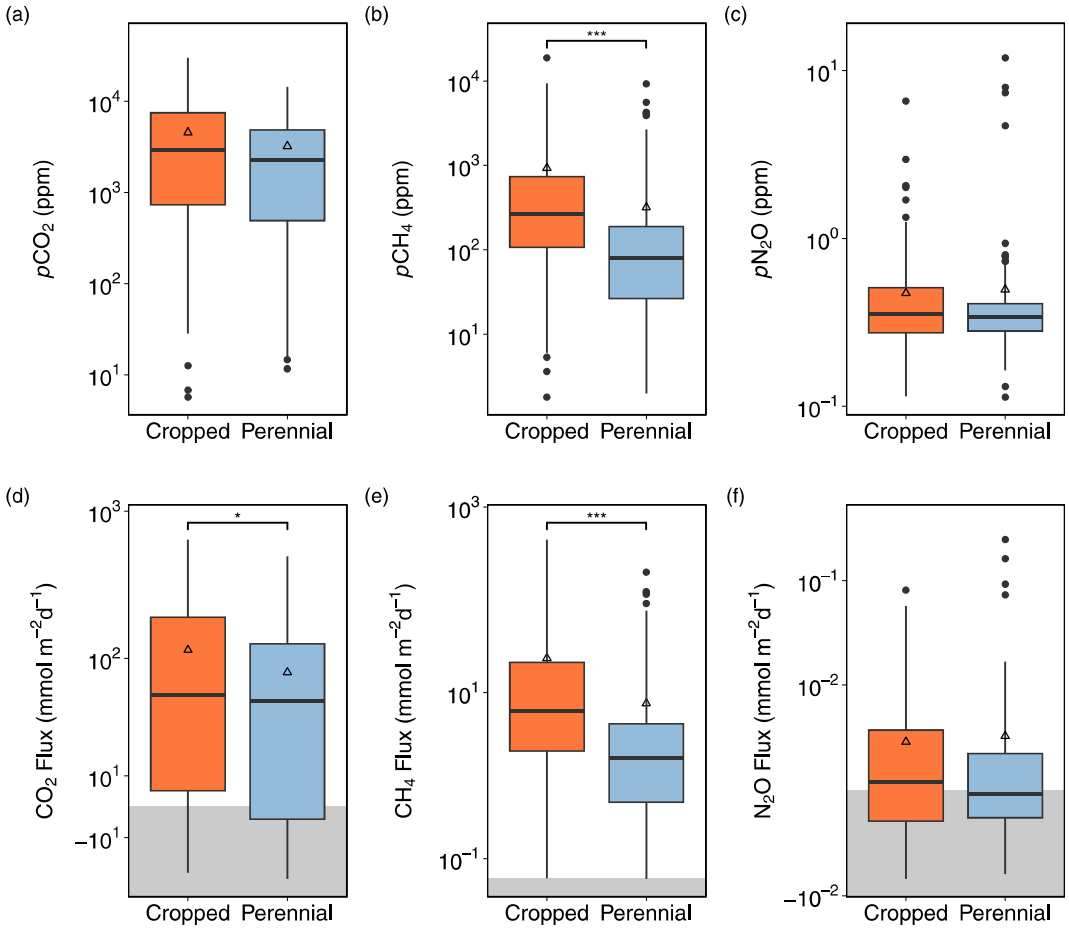

Figure 4. Partial pressure (a–c) and flux (d–f) for CO_2 (a, d), CH_4 (b, e), and N_2O (c, f) in wetlands by surrounding land use in the Canadian PPR. Fluxes (d–f) are plotted on a pseudo-log scale which gradually transitions to a linear scale around zero (Text S1 in Supporting Information S1). The horizontal line in each box represents the median value, the upper and lower ends of each box represent the first and third quartiles, respectively, and the whiskers represent the minimum and maximum values of the data set, excluding outliers. Outliers are plotted as black points. Empty triangles denote mean values. The shaded region represents a negative flux, in which GHG uptake occurs, and the unshaded region represents a positive flux in which GHGs are emitted to the atmosphere. Significance levels for either ANOVA (when meeting assumptions of normality and homogeneity of variances) or the Kruskal-Wallis test (when not) are shown as *, **, and *** for p values < 0.05, 0.01, and 0.001, respectively.

better predicted ($R^2 = 0.36$, Figure 7), predominantly by land use (+0.96, $p < 0.001$) and secondarily by historical agricultural suitability (−0.16, $p < 0.001$). Although cropland was also a significant predictor for PC3 (+0.22, $p = 0.033$), PC3 was still poorly predicted ($R^2 = 0.02$, Figure 7). Historical agricultural suitability significantly predicted land use, although the magnitude of the loading was small (−0.09, $p < 0.001$). PC1 (+DOC, $+NH_4^+$, +TDN) only had minor (<0.2) effects on any of the GHGs (Figure 7). Both pCO_2 and pN_2O were poorly predicted by all the principal components ($R^2 = 0.07$ and 0.01, respectively). pCO_2 was significantly explained by all three principal components (+0.11, +0.18, and −0.15, and $p = 0.007$, <0.001, and = 0.002, for PC1, PC2, and PC3, respectively). On the other hand, pCH_4 was well-predicted ($R^2 = 0.35$) by both PC1 and PC2, especially PC2 (+0.56, $p < 0.001$), which was the principal component most affected by cropland (Figure 7). Finally, the total instantaneous GHG flux ($R^2 = 0.53$) was most influenced by pCH_4 (+0.65, $p < 0.001$).

4. Discussion

Recent syntheses have highlighted the lack of knowledge about wetland disturbance and implications for regional to global emissions budgets (Drever et al., 2021; Kolka et al., 2018). Our study identified how agricultural land uses impact wetland aquatic GHG emissions, thereby addressing uncertainties around wetland emissions budgets

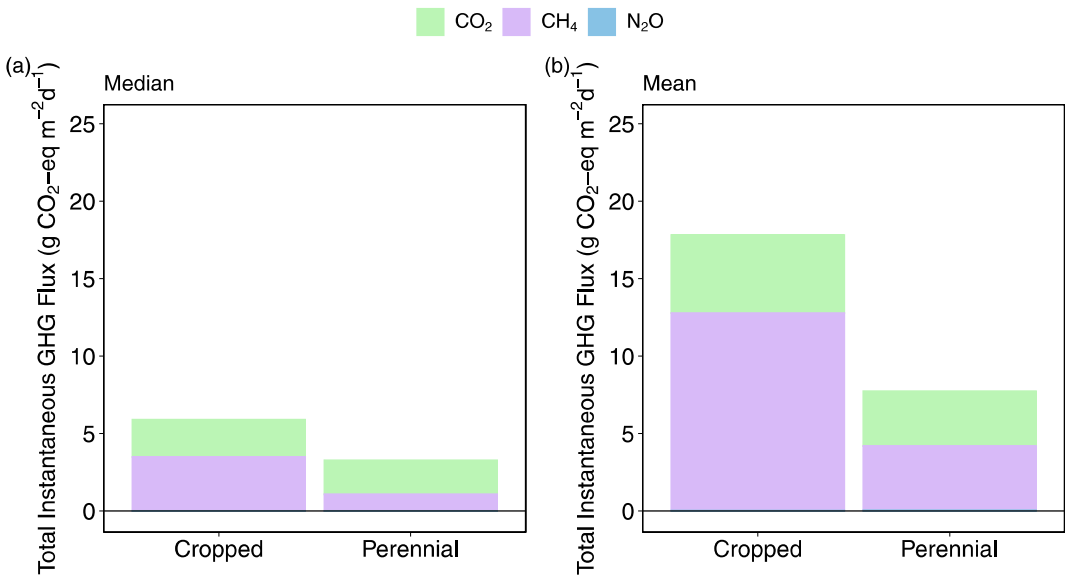

Figure 5. Median (a) and mean (b) total instantaneous GHG flux, in CO_2 equivalents on a 100-year time scale, by land use and the contributions of each GHG.

in the PPR. Specifically, we found that cropping practices appear to alter wetland water chemistry (Figures 2 and 3) and ecosystem functioning, causing a doubling of total wetland aquatic GHG emissions compared to wetlands in pasture and other perennially vegetated landscapes (Figures 4 and 5). By sampling all three major GHGs, we show distinct sensitivities of each gas to land use impacts (Figures 6 and 7). While aquatic N_2O emissions were negligible, CO_2 emissions were high but not strongly impacted by agricultural land use. Emissions of CH_4, on the other hand, were the largest contributor to total instantaneous diffusive GHG emissions on a 100-year time scale and were highly sensitive to surrounding land use (Figure 7). Increased CH_4 emissions alone caused most of the observed doubling in the total instantaneous GHG flux in wetlands within cropped landscapes (Figure 5). Overall, our findings help characterize the patterns and magnitude of agricultural impacts on wetland emissions in the PPR and may extend to other agricultural regions worldwide.

4.1. Land Use Impacts on Wetland Water Chemistry

Agricultural land use altered wetland water chemistry, likely through direct effects (i.e., fertilizer addition, crop nutrient uptake, and soil disturbance) and indirect effects (i.e., impacts on wetland redox conditions). Compared to wetlands embedded in perennially vegetated fields, cropped wetlands had elevated TP and NH_4^+ content (Figures 2 and 3, $p < 0.001$). Both nutrients are associated with the most applied forms of fertilizer in Canada (TP from monoammonium phosphate and NH_4^+ from monoammonium phosphate, urea, and urea ammonium nitrate; Agriculture, Food, and Rural Development, 2004; Statistics Canada, 2023). Cropped wetlands did not have elevated concentrations of other N species not typically added as fertilizer (e.g., NO_x), contrary to other studies in Saskatchewan (Bedard-Haughn et al., 2006). Indirect mechanisms may also elevate TP and NH_4^+ concentrations, such as agricultural influences on redox conditions. If nutrient additions enhance organic matter production in the water column and subsequent microbial decomposition and oxygen consumption in underlying sediments, then this shift in redox properties linked to O_2 depletion could facilitate the release of nutrients back to the water column. Specifically, under reducing conditions, chemically bound P is released as Fe^{3+} shifts to Fe^{2+} (Blomqvist et al., 2004; Gächter & Müller, 2003), and microbial decomposition of complex organics releases mineralized NH_4^+ (Halemejko & Chrost, 1986; Solomon et al., 2010; Wetzel, 2001). Importantly, the differences in TP and NH_4^+ content across land use persisted even when accounting for historical soil suitability for agriculture (Figure S6 in Supporting Information S1). This demonstrates that while the differences in wetland water quality between cropped and perennially covered landscapes partly depend on underlying differences in hydrology, topography, and soil chemistry that shape land management decisions (i.e., where to initiate cropping vs. grazing), water quality differences are clearly also linked to land use practices themselves that impact wetland nutrient content and trophic status.

19449224, 2025, 3, Downloaded from https://agupubs.onlinelibrary.wiley.com/doi/10.1029/2024GB008209 by University Of Lethbridge, Wiley Online Library on [09/07/2025]. See the Terms and Conditions (https://onlinelibrary.wiley.com/terms-and-conditions) on Wiley Online Library for rules of use; OA articles are governed by the applicable Creative Commons License

19449224, 2025, 3, Downloaded from https://agupubs.onlinelibrary.wiley.com/doi/10.1029/2024GB008209 by University Of Lethbridge, Wiley Online Library on [09/07/2025]. See the Terms and Conditions (https://onlinelibrary.wiley.com/terms-and-conditions) on Wiley Online Library for rules of use; OA articles are governed by the applicable Creative Commons License

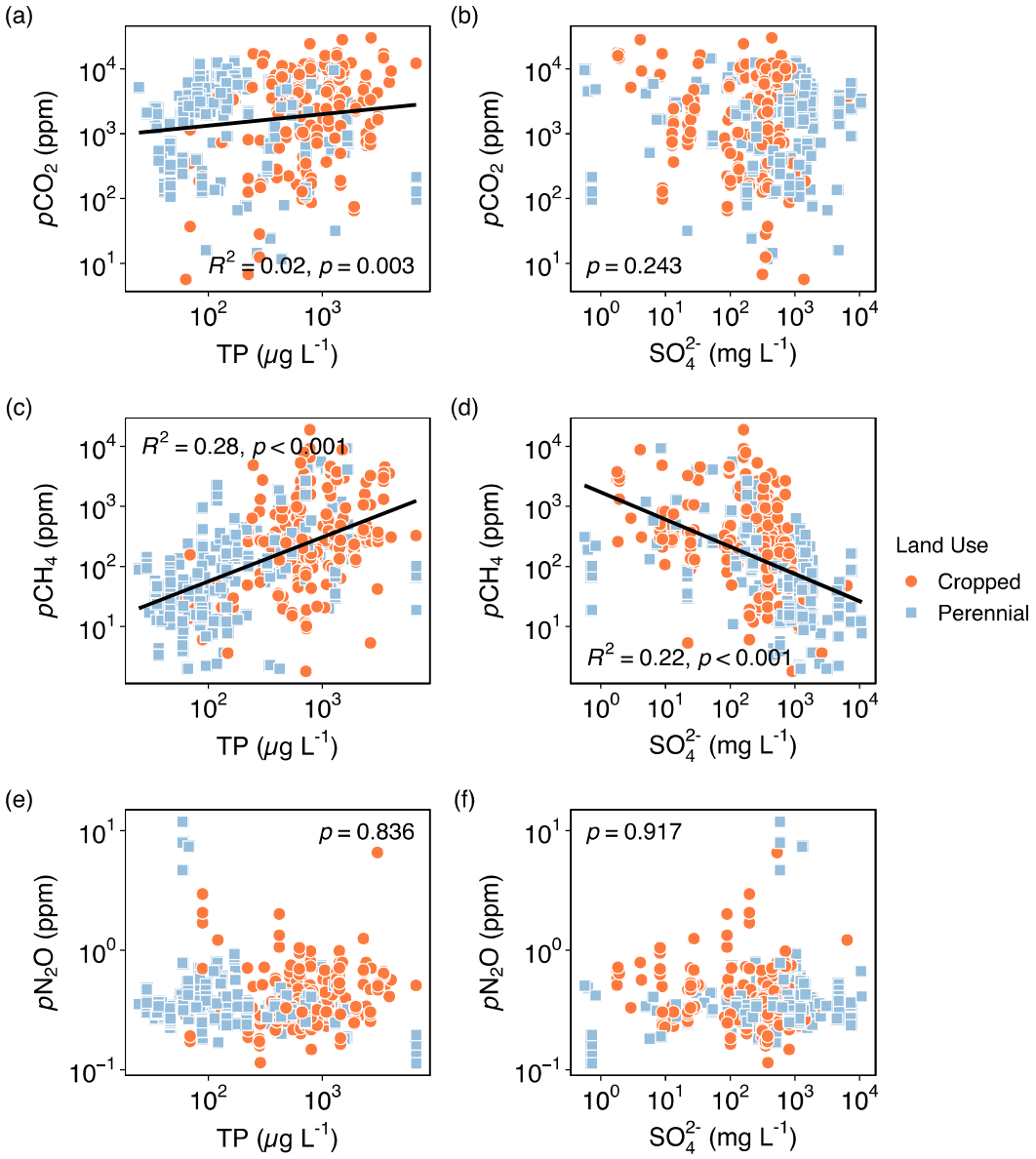

Figure 6. Partial pressure of CO_2 (a–b), CH_4 (c–d), and N_2O (e–f) versus TP (a, c, e) and SO_4^{2-} (b, d, f) in wetlands by surrounding land use in the Canadian PPR. All axes are log-scaled.

The nutrient requirements of crops versus pasture may differentially impact SO_4^{2-} concentrations, resulting in lower SO_4^{2-} concentrations in wetlands in cropland compared to perennial landscapes (Figures 2 and 3). Varieties of canola (e.g., *Brassica napus* L. or *Brassica rapa*), which is the crop with the second highest acreage in the Canadian Prairies (Malaj et al., 2020), have high S requirements (Jackson, 2000; Mbakwe & Adegeye, 2022). S deficiencies in Prairie soils are being exacerbated by increased production of canola, agricultural intensification, adoption of high yield cultivars, and decreased S deposition due to emissions controls (Feinberg et al., 2021; Grant et al., 2012). As a result, greater crop uptake of SO_4^{2-} in already S deficient soils could partially explain the lower SO_4^{2-} concentrations in wetlands within cropped landscapes (Figures 2 and 7: PC2). The range in SO_4^{2-} content may also be due to natural underlying differences in groundwater hydrology or soil salinity between cropped and grazed/perennially vegetated landscapes (Pennock et al., 2010), with greater delivery of SO_4^{2-} rich ground and surface water to wetlands in grazed landscapes. However, analysis of historical soil suitability for agriculture, which includes salinity (Table S3 in Supporting Information S1), showed no cases of high salinity limiting agricultural productivity in any of our sampled wetlands and there was no significant difference in the

19449224, 2025, 3, Downloaded from https://agupubs.onlinelibrary.wiley.com/doi/10.1029/2024GB008209 by University Of Lethbridge, Wiley Online Library on [09/07/2025]. See the Terms and Conditions (https://onlinelibrary.wiley.com/terms-and-conditions) on Wiley Online Library for rules of use; OA articles are governed by the applicable Creative Commons License

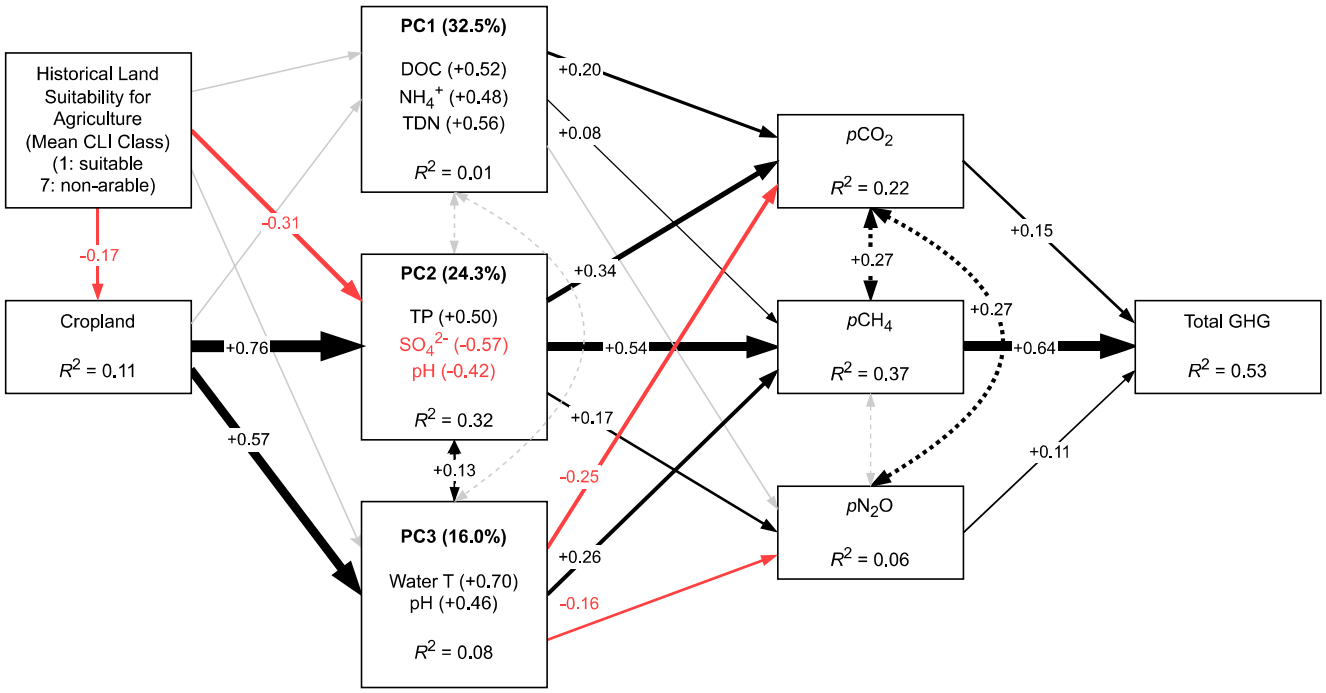

Figure 7. Structural equation model (SEM) demonstrating the controls on the partial pressures of the three major GHGs (pCO_2, pCH_4, and pN_2O), and ultimately the total instantaneous GHG flux ("Total GHG"), in CO_2 equivalents on a 100-year time scale. Each control is a principal component from Figure 2 and the loadings of the predominant variables for each component are listed. The principal components are influenced by land use, a categorical variable of cropland versus perennial cover (with the cropland relationships displayed) and historical land suitability for agriculture (CLI class). Black arrows represent positive effects, and red arrows represent negative effects. Gray arrows are non-significant effects ($p > 0.05$). Dashed arrows represent the residual covariance between variables. The standardized coefficients summarizing the effect sizes are denoted for each effect, and the arrow thickness is scaled to the effect magnitude.

distribution of soil suitability class or subclass across land use types (Table S1, Figure S5 in Supporting Information S1). Further, while SO_4^{2-} was significantly different across agricultural land suitability classifications, the differences across land use persisted even after accounting for historical soil differences (Figure S6a in Supporting Information S1, $p < 0.001$, two-way ANOVA vs. Figure 3, $p < 0.001$, one-way ANOVA). Thus, while we cannot definitively identify the causes of depleted SO_4^{2-} content in wetlands within cropped landscapes, SO_4^{2-} differences across land uses are, to some extent, driven by agricultural practices and not just underlying environmental differences. Together, these agriculturally driven changes in water chemistry likely explain a portion of the differences observed in wetland GHG emissions between land use categories.

4.2. Cropping Alters Nutrient and Redox Controls on Wetland CH_4 Emissions

The SEM points to temperature, eutrophication, and redox controls on total emissions largely through impacts on CH_4 content (Figure 7). Temperature controls on CH_4 production are well-documented, given the temperature-sensitivity of methanogenesis (Yvon-Durocher et al., 2014). While some variation in CH_4 was explained by temperature (Figure 7: PC3), it was not the strongest predictor, in line with recent work (Chang et al., 2021). Further, while ebullitive flux rates were not measured here, recent work on wetlands in the Canadian PPR has shown a weak relationship between temperature and CH_4 ebullition (Baron et al., 2022). Globally, CH_4 concentrations in lakes were positively associated with lake chlorophyll concentrations and trophic status (DelSontro et al., 2018), either through the creation of anoxic conditions during enhanced respiration of OC or because of an increase in labile C substrate for CH_4 production (West et al., 2012). Consistent with this observation for lakes, we found that pCH_4 was explained well by TP (Figures 6c and 7: PC2), which varied significantly across both historical soil suitability for agriculture and present-day land use category (Figures 2, 3, and 7: PC2). This relationship could be due to links between eutrophication and increased aquatic and vegetated zone primary production, which supplies OM to fuel CH_4 production (Badiou et al., 2019; Moss et al., 2011; Vachon et al., 2020). Conversely, the connection between elevated TP and CH_4 emissions may also be indirect, as the internal cycling of TP is also redox-sensitive, given its association with Fe in sediment (Karstens et al., 2015).

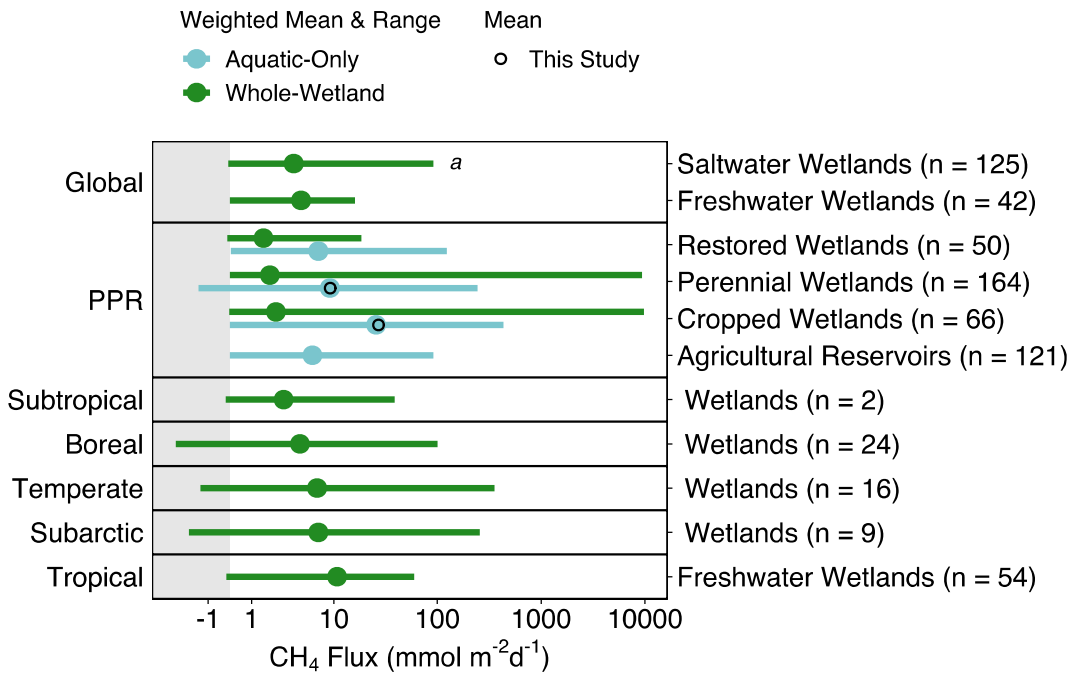

Figure 8. Comparison of diffusive CH_4 fluxes from wetlands in the PPR versus other regional and global[a] estimates; data sources are listed in Table S5 in Supporting Information S1. Filled circles are the weighted mean (blue = aquatic-only and green = whole-wetland) of methane fluxes, weighted by the number of sites included in each study's mean[b] (Table S5 in Supporting Information S1). The black empty circles for PPR perennial and cropped wetlands are the (unweighted) means calculated from this study. The total number of sites (n) included in the weighted means is listed for each wetland type and region. Lines represent the range for each system and region. Fluxes are plotted on a pseudo log-scale. [a] Global estimates for saltwater and freshwater wetlands include both diffusive and ebullitive CH_4 emissions. [b] Study means for whole-wetland perennial and cropland wetlands include the geometric means calculated from Bansal et al. (2023) instead of the arithmetic mean, as the arithmetic mean for this particular data set was skewed toward high values that were likely inclusive of ebullition.

Specifically, anoxic conditions that are ideal for methanogenesis may also promote P release from sediment. Increased SO_4^{2-} in freshwater has been associated with the release of P at sediment-water boundaries (Blomqvist et al., 2004; Chen et al., 2021). However, as TP and SO_4^{2-} were negatively correlated ($R^2 = 0.37$, $p < 0.001$, data not shown), it is unlikely that increased TP content is primarily a redox-driven sediment response, given that this mechanism would lead to a positive correlation between TP and SO_4^{2-} (Caraco et al., 1989). Instead, this points to external sources of TP (i.e., crop fertilizer) overwhelming the potential controls on internal P loading as the main driver of TP concentrations and enhanced CH_4 emissions. Therefore, nutrient loading from agricultural fertilizer runoff may increase CH_4 concentrations and fluxes in PPR wetlands through the production and degradation of labile C and the promotion of anoxia.

Land use impacts that support lower wetland SO_4^{2-} concentrations may also cause increased CH_4 content and emissions by altering redox conditions that control CH_4 production. Recent work showed that elevated salinity in hardwater shallow lentic systems in the PPR downregulates CH_4 diffusive and ebullitive emissions (Baron et al., 2022; Pennock et al., 2010; Soued et al., 2024), as SO_4^{2-} reduction dominates as the primary organic C remineralization pathway over methanogenesis (Dalcin Martins et al., 2017). The negative relationship observed here between pCH_4 and SO_4^{2} (Figures 6d and 7: PC2) therefore suggests a redox control on CH_4 production and/or oxidation that is a result of both underlying soil differences in soil chemical characteristics or hydrology and agricultural practices such as crop choice and nutrient requirements. Further work is required to differentiate the role of each (or additional) mechanism(s) linking SO_4^{2-} and CH_4 emissions across distinct agricultural land uses.

4.3. Enhanced Aquatic CH_4 Emissions From Cropped Landscapes

The rates of diffusive aquatic CH_4 emissions from wetlands in cropped landscapes reported here (mean = 23.4, range = −0.002 to 445.1 mmol m^{-2} d^{-1}) are higher than for other wetlands (Figure 8, Table S5 in Supporting

19449224, 2025, 3, Downloaded from https://agupubs.onlinelibrary.wiley.com/doi/10.1029/2024GB008209 by University Of Lethbridge, Wiley Online Library on [09/07/2025]. See the Terms and Conditions (https://onlinelibrary.wiley.com/terms-and-conditions) on Wiley Online Library for rules of use; OA articles are governed by the applicable Creative Commons License

19449224, 2025, 3, Downloaded from https://agupubs.onlinelibrary.wiley.com/doi/10.1029/2024GB008209 by University Of Lethbridge, Wiley Online Library on [09/07/2025]. See the Terms and Conditions (https://onlinelibrary.wiley.com/terms-and-conditions) on Wiley Online Library for rules of use; OA articles are governed by the applicable Creative Commons License

Information S1). The mean diffusive aquatic CH_4 flux from wetlands in perennial landscapes in this study (mean = 7.7, range = −0.005 to 198.1 mmol m^{-2} d^{-1}) was similar to other estimates for wetlands in perennially vegetated landscapes of the PPR (Table S5 in Supporting Information S1). On average, whole-wetland diffusive CH_4 emissions from perennially vegetated PPR wetlands were on the low end of global diffusive and ebullitive wetland emissions and similar in magnitude to diffusive fluxes from subtropical wetlands (Figure 8, Table S5 in Supporting Information S1). However, the variability of PPR whole-wetland CH_4 emissions was higher than any other system (Figure 8), which could be because chamber measurements of CH_4 fluxes from Bansal et al. (2023) may include ebullition, which can range in flux rate from 0.0005 to >40 mmol m^{-2} d^{-1} for PPR wetlands (Baron et al., 2022). To overcome this issue, we calculated the geometric means of flux rates reported for that study (Bansal et al., 2023) rather than arithmetic means (Table S5 in Supporting Information S1), thereby minimizing the influence of extreme flux rates that likely do not reflect diffusive emissions. The low mean whole-wetland diffusive CH_4 emissions (~2 mmol m^{-2} d^{-1}) of perennial wetlands in the PPR (Figure 8, Table S5 in Supporting Information S1) could be due to relatively high SO_4^{2-} concentrations (Table S4 in Supporting Information S1), which restricts the rate of CH_4 production and can enhance oxidation (Soued et al., 2024). Thus, PPR whole-wetland CH_4 emissions may be lower than in other regions.

Clearly, knowledge of local agricultural land use can provide context to help explain why regional CH_4 emissions measured here exceed the values expected for natural systems. But a large degree of uncertainty remains for regional wetland CH_4 emissions estimates. Mean aquatic diffusive CH_4 emissions from wetlands in cropped landscapes were higher than those from all other wetlands (both natural perennial and restored) and agricultural reservoirs in the PPR (Figure 8). This is also line with previous work; in the subtropics, wetlands embedded in "agronomically improved" landscapes (nutrient-amended, heavily grazed, and replaced native grasses with non-native forage grasses) had more than double the diffusive aquatic methane emissions than wetlands in semi-native landscapes (2.82 vs. 0.75 μmol m^{-2} s^{-1}) (DeLucia et al., 2019). Additionally, agricultural ditches in the North China Plain had 12 times higher CH_4 emissions than nearby streams, which was attributed to agricultural nutrient loading (Wu et al., 2023). Interestingly, these findings of greater CH_4 emissions in agricultural wetlands did not hold true for combined rates from emergent vegetation and aquatic habitats, as whole-wetland CH_4 emissions were higher in perennial wetlands than cropped wetlands (Figure 8, Table S5 in Supporting Information S1). However, we caution this interpretation as the mean for perennial wetlands is driven by observations from a single study (Bansal et al., 2023; Table S5 in Supporting Information S1), whereas another study showed greater whole wetland emissions in cropped landscapes compared to perennially vegetated habitat (Table S5 in Supporting Information S1, Gleason et al., 2009). In addition to this variability among studies, accounting for the different emissions pathways adds further uncertainty to our ability to estimate whole-wetland CH_4 emissions. Averaging CH_4 emissions across both the open water and vegetated zones in our wetlands (as done by Bansal et al., 2023) would lower the estimates of whole-ecosystem diffusive emissions, while including ebullitive fluxes would increase emissions. The rate of ebullition is difficult to predict for our wetlands individually, though previously reported values are similar in magnitude (with a wider range) to diffusive emissions. Baron et al. (2022) reported values for PPR wetlands of 0.0005 to >40 mmol m^{-2} d^{-1} (mean ~ 12–22 mmol m^{-2} d^{-1}), while Soued et al. (2024) reported summertime values for PPR wetlands and agricultural reservoirs of 0.000002–4.7 mmol m^{-2} d^{-1} (mean ~ 0.9 mmol m^{-2} d^{-1}). While ebullitive fluxes are lower in more saline SO_4^{2-} rich systems (Baron et al., 2022; Soued et al., 2024), our ability to predict these fluxes across systems and regions is weak, and should be the focus of future work. Regardless, our results placed in the context of existing findings confirm that aquatic emissions are the dominant term in wetland CH_4 budgets, and that open water emissions are enhanced in cropped landscapes relative to natural systems.

4.4. CO_2 Fluxes and Drivers

Carbon dioxide emissions from this study were comparable to other wetland open water habitats, but high for eutrophic inland waters. On average, the CO_2 flux rate was positive (97.3 ± 125.3 mmol m^{-2} d^{-1}), signifying that the open water portions of the prairie wetlands studied here predominantly emitted CO_2 to the atmosphere (Figure 4d, Table S4 in Supporting Information S1), in line with observations from other prairie wetlands (Bortolotti et al., 2016; Jensen et al., 2023). The CO_2 fluxes reported here were similar to those reported for subarctic ponds and saline lakes (averaging ~100–200 mmol m^{-2} d^{-1}) but were high compared to most lakes and reservoirs (averaging ~ 0–100 mmol m^{-2} d^{-1}) (Bortolotti et al., 2016 and references therein). This is notable given that nutrient loading in lakes often reduces lake CO_2 emissions or even acts as a CO_2 sink by stimulating

19449224, 2025, 3, Downloaded from https://agupubs.onlinelibrary.wiley.com/doi/10.1029/2024GB008209 by University Of Lethbridge, Wiley Online Library on [09/07/2025]. See the Terms and Conditions (https://onlinelibrary.wiley.com/terms-and-conditions) on Wiley Online Library for rules of use; OA articles are governed by the applicable Creative Commons License

autotrophic CO_2 uptake (Beaulieu et al., 2019; DelSontro et al., 2018; Vachon et al., 2020). Our findings therefore highlight the differences between eutrophic prairie wetlands and other eutrophic aquatic habitats, suggesting the potentially unique drivers of CO_2 fluxes in PPR wetlands.

The weak positive relationship between CO_2 emissions and both nutrient and organic matter content (Figures 6a, 6b, and 7) suggests that while heterotrophic metabolism sustains aquatic emissions, other factors including autochthonous production and carbonate buffering in these highly alkaline systems decouple metabolism and CO_2. Positive relationships between pCO_2, nutrient concentrations, and DOC were previously shown to reflect external organic inputs that fuel aquatic metabolism and CO_2 emissions in boreal aquatic systems (Lapierre et al., 2013). Conversely, in the PPR wetlands studied here, PC1 (+DOC, $+NH_4^+$, and +TDN) was very weakly related to pCO_2 (Figure 7). While microbial (Dalcin Martins et al., 2017; Waiser & Robarts, 2004) and photochemical oxidation (Waiser & Robarts, 2004) of DOC is often intense, these processes were not clearly linked to gradients of CO_2 emissions across systems, as was also observed in other PPR wetlands (Bortolotti et al., 2016). This could be related to autochthonous OC production consuming CO_2 (Bortolotti et al., 2019). Further, although we cannot assess it directly as we lack alkalinity data, carbonate buffering is likely exerting an important influence on CO_2 emission patterns (Bortolotti et al., 2016; Stets et al., 2017) because at pH greater than 8, dissolved CO_2 is ionized to HCO_3^- (Butler, 1991). Our study systems were predominantly alkaline: pH was >8 for 85% of samples (median pH = 8.7; Figure 3). Thus, while the relationship between CO_2 and pH is bidirectional, reflecting in part the effect of photosynthesis and microbial CO_2 production on pH, carbonate buffering from external alkalinity inputs decouples the pCO_2-metabolism relationship and no clear patterns emerge across agricultural land use.

4.5. N_2O Fluxes and Drivers

Overall, open water mean N_2O fluxes were approximately 0 (Figure 4) and were negligible to the total instantaneous GHG flux in CO_2 equivalents (Figure 5). This is consistent with past work demonstrating that the highest wetland N_2O emissions occurred in moderately saturated wetland soils (Bedard-Haughn et al., 2006; Creed et al., 2013), and that, on average, the ponded, open water portion of wetlands and reservoirs had negligible N_2O fluxes (Chan et al., 2024; Tangen & Bansal, 2019) or were N_2O sinks (Aho et al., 2023; Soued et al., 2016; Webb, Hayes, et al., 2019). However, N_2O fluxes have been shown to be highly variable both spatially and temporally, and hotspots of N_2O emissions can be important. In U.S. prairie open water wetlands, Tangen and Bansal (2022) found two orders of magnitude higher N_2O fluxes in April compared to the rest of the ice-free period, suggesting a seasonal effect on N_2O production, consumption, or transport in ponded wetlands. This finding is reflected in our anomalously high N_2O fluxes from Saskatchewan and Alberta prairie wetlands in May compared with the other ice-free months (data not shown). While we are unsure what caused this pattern and do not have the required data to elucidate the mechanism, this observation helps establish the temporal patterns of open water N_2O emissions in PPR wetlands. Even accounting for these temporal spikes in emissions, the contributions of N_2O to the total GHG flux were negligible for open water wetlands (Figure 5).

N_2O was poorly predicted by environmental variables and not related to agricultural land use, suggesting complex drivers. Higher N_2O concentrations were found to be associated with NH_4^+ and NO_2^- enrichment in small tropical reservoirs (Wang et al., 2017) and prairie wetland soils (Bedard-Haughn et al., 2006), whereas other studies have found no or weak relationships between N_2O and DIN or nutrients (Chan et al., 2024; Webb, Hayes, et al., 2019). This could be because of nonlinear relationships between N_2O concentrations and DIN, with stratification modulating the effects of DIN on N_2O (Webb et al., 2021), or because complete denitrification to N_2 might be dominating over N_2O production, as was observed in coastal plain agricultural wetland soils (Morse & Bernhardt, 2013) and highly saturated agricultural soils (Ciarlo et al., 2008). In our systems, pN_2O was not well-predicted by any of the principal components (Figure 7, $R^2 = 0.01$) or any of the variables most affected by land use (Figures 6e and 6f). Thus, agricultural land use had no significant impact on open water N_2O emissions.

5. Conclusions

Here we showed that in the PPR, aquatic CH_4 emissions were greater from wetlands in cropped landscapes than perennially vegetated landscapes, due to land use impacts that increased aquatic P content and decreased SO_4^{2-} content. This means that changes to agricultural management practices such as P reduction and S addition may reduce open water wetland GHG emissions. Additional work is needed to elucidate the specific mechanisms by

19449224, 2025, 3, Downloaded from https://agupubs.onlinelibrary.wiley.com/doi/10.1029/2024GB008209 by University Of Lethbridge, Wiley Online Library on [09/07/2025]. See the Terms and Conditions (https://onlinelibrary.wiley.com/terms-and-conditions) on Wiley Online Library for rules of use; OA articles are governed by the applicable Creative Commons License

which agriculture changes wetland water quality (e.g., redox impacts, organic matter lability) in order to extend the findings from this study to other regions and to changing future land use scenarios.

While total aquatic GHG emissions rates measured here are greater than past estimates from non-agricultural land covers within the PPR, this may not be the case for whole-wetland emissions, which were low in the PPR compared to other wetlands globally. Further work is needed to evaluate drivers and trends at the whole-wetland scale (i.e., including both open water and emergent vegetation zones, and diffusive and ebullitive emissions). While including emergent vegetation zones in whole-wetland GHG estimates may lower average CH_4 emissions estimates from wetlands in cropped settings below those in perennially vegetated settings (Figure 8, Table S5 in Supporting Information S1), including CH_4 ebullition rates may offset this pattern as these fluxes tend to be higher than diffusive emissions (Badiou et al., 2011; Baron et al., 2022). Together, this has unclear implications for the total wetland GHG flux and C storage potential of wetlands in cropped versus perennially vegetated settings. Overall, our study fills a critical knowledge gap in the measurement and prediction of aquatic GHG emissions from agricultural wetlands in a region with one of the greatest wetland densities globally. Our work also provides information to assist agricultural managers to minimize wetland GHG emissions.

Data Availability Statement

Data from this manuscript are openly accessible through the Federated Research Data Repository (Bogard et al., 2025).

Acknowledgments
We would like to thank members of the Bogard Lab and colleagues at Ducks Unlimited Canada for their assistance with field data collection. We also thank Llwellyn Armstrong and Dr. Sam Woodman for suggestions regarding statistical analysis. Funds supporting this work were obtained from multiple sources. MJB was funded by awards from the University of Lethbridge, NSERC, Canada Foundation for Innovation (CFI) and the Canada Research Chairs (CRC) program. CS was supported by a MITACS-Accelerate grant with Ducks Unlimited Canada in collaboration with LEB and MJB, and a postdoctoral fellowship from the National Scientific and Engineering Research Council (NSERC). LEB and PB were supported by Ducks Unlimited Canada's Institute for Wetland and Waterfowl Research. PB was funded by the Beef Cattle Research Council, Ag Action Manitoba, and an NSERC Alliance grant.

References

Agriculture, Food, & Rural Development. (2004). *Alberta fertilizer guide* (p. 541–1). Agri-Facts, Agdex.

Agriculture and Agri-Food Canada. (1998). Canada Land Inventory, National Soil DataBase [Dataset]. Retrieved from https://sis.agr.gc.ca/cansis/nsdb/cli/index.html

Aho, K. S., Maavara, T., Cawley, K. M., & Raymond, P. A. (2023). Inland waters can act as nitrous oxide sinks: Observation and modeling reveal that nitrous oxide undersaturation may partially offset emissions. *Geophysical Research Letters*, *50*(21), e2023GL104987. https://doi.org/10.1029/2023GL104987

Allen, S. J., & Hubbard, R. (1986). Regression equations for the latent roots of random data correlation matrices with unities on the diagonal. *Multivariate Behavioral Research*, *21*, 393–398.

Apple, J. K., del Giorgio, P. A., & Kemp, W. M. (2006). Temperature regulation of bacterial production, respiration, and growth efficiency in a temperate salt-marsh estuary. *Aquatic Microbial Ecology*, *43*(3), 243–254. https://doi.org/10.3354/ame043243

Badiou, P., McDougal, R., Pennock, D., & Clark, B. (2011). Greenhouse gas emissions and carbon sequestration potential in restored wetlands of the Canadian prairie pothole region. *Wetlands Ecology and Management*, *19*(3), 237–256. https://doi.org/10.1007/s11273-011-9214-6

Badiou, P., Page, B., & Ross, L. (2019). A comparison of water quality and greenhouse gas emissions in constructed wetlands and conventional retention basins with and without submerged macrophyte management for storm water regulation. *Ecological Engineering*, *127*, 292–301. https://doi.org/10.1016/j.ecoleng.2018.11.028

Balmer, M., & Downing, J. (2011). Carbon dioxide concentrations in eutrophic lakes: Undersaturation implies atmospheric uptake. *Inland Waters*, *1*(2), 125–132. https://doi.org/10.5268/IW-1.2.366

Bansal, S., Post van der Burg, M., Fern, R. R., Jones, J. W., Lo, R., McKenna, O. P., et al. (2023). Large increases in methane emissions expected from North America's largest wetland complex. *Science Advances*, *9*(eade1112), 1–14. https://doi.org/10.1126/sciadv.ade1112

Baron, A. A. P., Dyck, L. T., Amjad, H., Bragg, J., Kroft, E., Newson, J., et al. (2022). Differences in ebullitive methane release from small, shallow ponds present challenges for scaling. *Science of the Total Environment*, *802*, 149685. https://doi.org/10.1016/j.scitotenv.2021.149685

Beaulieu, J. J., DelSontro, T., & Downing, J. A. (2019). Eutrophication will increase methane emissions from lakes and impoundments during the 21st century. *Nature Communications*, *10*(1375), 1–5. https://doi.org/10.1038/s41467-019-09100-5

Beaulieu, J. J., Tank, J. L., Hamilton, S. K., Wollheim, W. M., Hall, R. O., Mulholland, P. J., et al. (2011). Nitrous oxide emission from denitrification in stream and river networks. *Proceedings of the National Academy of Sciences of the United States of America*, *108*(1), 214–219. https://doi.org/10.1073/pnas.1011464108

Bedard-Haughn, A., Matson, A. L., & Pennock, D. J. (2006). Land use effects on gross nitrogen mineralization, nitrification, and N_2O emissions in ephemeral wetlands. *Soil Biology and Biochemistry*, *38*(12), 3398–3406. https://doi.org/10.1016/j.soilbio.2006.05.010

Blomqvist, S., Gunnars, A., & Elmgren, R. (2004). Why the limiting nutrient differs between temperate coastal seas and freshwater lakes: A matter of salt. *Limnology & Oceanography*, *49*(6), 2236–2241. https://doi.org/10.4319/lo.2004.49.6.2236

Bogard, M. J., Badiou, P., Bortolotti, L. E., Kowal, P., Logozzo, L. A., & Page, B. (2025). Dataset for Logozzo et al. Global Biogeochemical Cycles, "Agricultural land use impacts aquatic greenhouse gas emissions from wetlands in the Canadian Prairie Pothole Region." [Dataset]. *Federated Research Data Repository*. https://doi.org/10.20383/103.01204

Bortolotti, L. E., St. Louis, V. L., & Vinebrooke, R. D. (2019). Drivers of ecosystem metabolism in restored and natural prairie wetlands. *Canadian Journal of Fisheries and Aquatic Sciences*, *76*(12), 2396–2407. https://doi.org/10.1139/cjfas-2018-0419

Bortolotti, L. E., St. Louis, V. L., Vinebrooke, R. D., & Wolfe, A. P. (2016). Net ecosystem production and carbon greenhouse gas fluxes in three prairie wetlands. *Ecosystems*, *19*(3), 411–425. https://doi.org/10.1007/s10021-015-9942-1

Burgin, A. J., & Hamilton, S. K. (2007). Have we overemphasized the role of denitrification in aquatic ecosystems? A review of nitrate removal pathways. *Frontiers in Ecology and the Environment*, *5*(2), 89–96. https://doi.org/10.1890/1540-9295(2007)5[89:HWOTRO]2.0.CO;2

Burgin, A. J., Yang, W. H., Hamilton, S. K., & Silver, W. L. (2011). Beyond carbon and nitrogen: How the microbial energy economy couples elemental cycles in diverse ecosystems. *Frontiers in Ecology and the Environment*, *9*(1), 44–52. https://doi.org/10.1890/090227

Butler, J. N. (1991). *Carbon dioxide equilibria and their applications*. Routledge. https://doi.org/10.1201/9781315138770

Caraco, N. F., Cole, J. J., & Likens, G. E. (1989). Evidence for sulphate-controlled phosphorus release from sediments of aquatic systems. *Nature*, *341*(6240), 316–318. https://doi.org/10.1038/341316a0

Chan, C. N., Gushulak, C. A. C., Leavitt, P. R., Logozzo, L. A., Finlay, K., & Bogard, M. J. (2024). Experimental ecosystem eutrophication causes offsetting effects on emissions of CO_2, CH_4, and N_2O from agricultural reservoirs. *Environmental Science and Technology*, *58*(16), 7045–7055. https://doi.org/10.1021/acs.est.3c07520

Chang, K.-Y., Riley, W. J., Knox, S. H., Jackson, R. B., McNicol, G., Poulter, B., et al. (2021). Substantial hysteresis in emergent temperature sensitivity of global wetland CH_4 emissions. *Nature Communications*, *12*(1), 2266. https://doi.org/10.1038/s41467-021-22452-1

Chen, J., Zhang, H., Liu, L., Zhang, J., Cooper, M., Mortimer, R. J. G., & Pan, G. (2021). Effects of elevated sulfate in eutrophic waters on the internal phosphate release under oxic conditions across the sediment-water interface. *Science of the Total Environment*, *790*, 148010. https://doi.org/10.1016/j.scitotenv.2021.148010

Ciarlo, E., Conti, M., Bartoloni, N., & Rubio, G. (2008). Soil N_2O emissions and $N_2O/(N_2O+N_2)$ ratio as affected by different fertilization practices and soil moisture. *Biology and Fertility of Soils*, *44*(7), 991–995. https://doi.org/10.1007/s00374-008-0302-6

Cole, J. J., & Caraco, N. F. (1998). Atmospheric exchange of carbon dioxide in a low-wind oligotrophic lake measured by the addition of SF6. *Limnology & Oceanography*, *43*(4), 647–656. https://doi.org/10.4319/lo.1998.43.4.0647

Conly, F. M., & van der Kamp, G. (2001). Monitoring the hydrology of Canadian prairie wetlands to detect the effects of climate change and land use changes. *Environmental Monitoring and Assessment*, *67*(1), 195–215. https://doi.org/10.1023/A:1006486607040

Creed, I. F., Miller, J., Aldred, D., Adams, J. K., Spitale, S., & Bourbonniere, R. A. (2013). Hydrologic profiling for greenhouse gas effluxes from natural grasslands in the prairie pothole region of Canada. *Journal of Geophysical Research: Biogeosciences*, *118*(2), 680–697. https://doi.org/10.1002/jgrg.20050

Dalcin Martins, P., Hoyt, D. W., Bansal, S., Mills, C. T., Tfaily, M., Tangen, B. A., et al. (2017). Abundant carbon substrates drive extremely high sulfate reduction rates and methane fluxes in Prairie Pothole Wetlands. *Global Change Biology*, *23*(8), 3107–3120. https://doi.org/10.1111/gcb.13633

DelSontro, T., Beaulieu, J. J., & Downing, J. A. (2018). Greenhouse gas emissions from lakes and impoundments: Upscaling in the face of global change. *Limnology and Oceanography Letters*, *3*(3), 64–75. https://doi.org/10.1002/lol2.10073

DelSontro, T., Boutet, L., St-Pierre, A., del Giorgio, P. A., & Prairie, Y. T. (2016). Methane ebullition and diffusion from northern ponds and lakes regulated by the interaction between temperature and system productivity. *Limnology & Oceanography*, *61*(S1), S62–S77. https://doi.org/10.1002/lno.10335

DeLucia, N. J., Gomez-Casanovas, N., Boughton, E. H., & Bernacchi, C. J. (2019). The role of management on methane emissions from subtropical wetlands embedded in agricultural ecosystems. *Journal of Geophysical Research: Biogeosciences*, *124*(9), 2694–2708. https://doi.org/10.1029/2019JG005132

Drever, C. R., Cook-Patton, S. C., Akhter, F., Badiou, P. H., Chmura, G. L., Davidson, S. J., et al. (2021). Natural climate solutions for Canada. *Science Advances*, *7*(23), 1–13. https://doi.org/10.1126/sciadv.abd6034

Environment and Climate Change Canada. (2022). 2030 emissions reduction plan: Canada's next steps for clean air and a strong economy. Gatineau QC K1A 0H3. Retrieved from https://publications.gc.ca/collections/collection_2022/eccc/En4-460-2022-eng.pdf

Environment Canada. (1986). *Wetlands in canada: A valuable resource (Fact Sheet No. 86–4)* (p. 4). Lands Directorate. Retrieved from https://publications.gc.ca/collections/Collection/CW69-10-1999-1E.pdf

Euliss, N. H., Gleason, R. A., Olness, A., McDougal, R. L., Murkin, H. R., Robarts, R. D., et al. (2006). North American prairie wetlands are important nonforested land-based carbon storage sites. *Science of the Total Environment*, *361*(1), 179–188. https://doi.org/10.1016/j.scitotenv.2005.06.007

Feinberg, A., Stenke, A., Peter, T., Hinckley, E.-L. S., Driscoll, C. T., & Winkel, L. H. E. (2021). Reductions in the deposition of sulfur and selenium to agricultural soils pose risk of future nutrient deficiencies. *Communications Earth & Environment*, *2*(1), 1–8. https://doi.org/10.1038/s43247-021-00172-0

Fluet-Chouinard, E., Stocker, B. D., Zhang, Z., Malhotra, A., Melton, J. R., Poulter, B., et al. (2023). Extensive global wetland loss over the past three centuries. *Nature*, *614*(7947), 281–286. https://doi.org/10.1038/s41586-022-05572-6

Gächter, R., & Müller, B. (2003). Why the phosphorus retention of lakes does not necessarily depend on the oxygen supply to their sediment surface. *Limnology & Oceanography*, *48*(2), 929–933. https://doi.org/10.4319/lo.2003.48.2.0929

Gauci, V., Matthews, E., Dise, N., Walter, B., Koch, D., Granberg, G., & Vile, M. (2004). Sulfur pollution suppression of the wetland methane source in the 20th and 21st centuries. *Proceedings of the National Academy of Sciences of the United States of America*, *101*(34), 12583–12587. https://doi.org/10.1073/pnas.0404412101

Gleason, R. A., Tangen, B. A., Browne, B. A., & Euliss, N. H. (2009). Greenhouse gas flux from cropland and restored wetlands in the Prairie Pothole Region. *Soil Biology and Biochemistry*, *41*(12), 2501–2507. https://doi.org/10.1016/j.soilbio.2009.09.008

Goldhaber, M. B., Mills, C. T., Morrison, J. M., Stricker, C. A., Mushet, D. M., & LaBaugh, J. W. (2014). Hydrogeochemistry of Prairie Pothole Region wetlands: Role of long-term critical zone processes. *Chemical Geology*, *387*, 170–183. https://doi.org/10.1016/j.chemgeo.2014.08.023

Grant, C. A., Mahli, S. S., & Karamanos, R. E. (2012). Sulfur management for rapeseed. *Field Crops Research*, *128*, 119–128. https://doi.org/10.1016/j.fcr.2011.12.018

Griscom, B. W., Adams, J., Ellis, P. W., Houghton, R. A., Lomax, G., Miteva, D. A., et al. (2017). Natural climate solutions. *Proceedings of the National Academy of Sciences of the United States of America*, *114*(44), 11645–11650. https://doi.org/10.1073/pnas.1710465114

Gudasz, C., Bastviken, D., Steger, K., Premke, K., Sobek, S., & Tranvik, L. J. (2010). Temperature-controlled organic carbon mineralization in lake sediments. *Nature*, *466*(7305), 478–481. https://doi.org/10.1038/nature09186

Halemejko, G. Z., & Chrost, R. J. (1986). Enzymatic hydrolysis of proteinaceous particulate and dissolved material in an eutrophic lake. *Archiv für Hydrobiologie*, *107*, 1–21. https://doi.org/10.1127/archiv-hydrobiol/107/1986/1

Jackson, G. D. (2000). Effects of nitrogen and sulfur on canola yield and nutrient uptake. *Agronomy Journal*, *92*(4), 644–649. https://doi.org/10.2134/agronj2000.924644x

Jähne, B., Münnich, K. O., Bösinger, R., Dutzi, A., Huber, W., & Libner, P. (1987). On the parameters influencing air-water gas exchange. *Journal of Geophysical Research*, *92*(C2), 1937–1949. https://doi.org/10.1029/JC092iC02p01937

Jensen, S. A., Webb, J. R., Simpson, G. L., Baulch, H. M., Leavitt, P. R., & Finlay, K. (2023). Differential controls of greenhouse gas (CO_2, CH_4, and N_2O) concentrations in natural and constructed agricultural waterbodies on the northern great plains. *Journal of Geophysical Research: Biogeosciences*, *128*(4), e2022JG007261. https://doi.org/10.1029/2022JG007261

Karstens, S., Buczko, U., & Glatzel, S. (2015). Phosphorus storage and mobilization in coastal Phragmites wetlands: Influence of local-scale hydrodynamics. *Estuarine, Coastal and Shelf Science*, *164*, 124–133. https://doi.org/10.1016/j.ecss.2015.07.014

Klaus, M., & Vachon, D. (2020). Challenges of predicting gas transfer velocity from wind measurements over global lakes. *Aquatic Sciences*, *82*(3), 53. https://doi.org/10.1007/s00027-020-00729-9

19449224, 2025, 3, Downloaded from https://agupubs.onlinelibrary.wiley.com/doi/10.1029/2024GB008209 by University Of Lethbridge, Wiley Online Library on [09/07/2025]. See the Terms and Conditions (https://onlinelibrary.wiley.com/terms-and-conditions) on Wiley Online Library for rules of use; OA articles are governed by the applicable Creative Commons License

Kolka, R., Trettin, C., Tang, W., Krauss, K., Bansal, S., Drexler, J., et al. (2018). Chapter 13: Terrestrial wetlands. In *Second state of the carbon cycle report*. U.S. Global Change Research Program. https://doi.org/10.7930/SOCCR2.2018.Ch13

Krüger, M., Frenzel, P., & Conrad, R. (2001). Microbial processes influencing methane emission from rice fields. *Global Change Biology*, *7*(1), 49–63. https://doi.org/10.1046/j.1365-2486.2001.00395.x

Lapierre, J.-F., Guillemette, F., Berggren, M., & del Giorgio, P. A. (2013). Increases in terrestrially derived carbon stimulate organic carbon processing and CO_2 emissions in boreal aquatic ecosystems. *Nature Communications*, *4*(1), 2972. https://doi.org/10.1038/ncomms3972

Ledwell, J. J. (1984). The variation of the gas transfer coefficient with molecular diffusivity. In W. Brutsaert (Ed.), *Gas transfer at water surfaces* (pp. 293–302). D. Reidel.

Longman, R. S., Cota, A. A., Holden, R. R., & Fekken, G. C. (1989). A regression equation for the parallel analysis criterion in principal components analysis: Mean and 95th percentile eigenvalues. *Multivariate Behavioral Research*, *24*(1), 59–69. https://doi.org/10.1207/s15327906mbr2401_4

Malaj, E., Freistadt, L., & Morrissey, C. A. (2020). Spatio-temporal patterns of crops and agrochemicals in Canada over 35 years. *Frontiers in Environmental Science*, *8*. https://doi.org/10.3389/fenvs.2020.556452

Martinez-Cruz, K., Sepulveda-Jauregui, A., Casper, P., Anthony, K. W., Smemo, K. A., & Thalasso, F. (2018). Ubiquitous and significant anaerobic oxidation of methane in freshwater lake sediments. *Water Research*, *144*, 332–340. https://doi.org/10.1016/j.watres.2018.07.053

Mbakwe, I., & Adegeye, O. (2022). Yield and quality response of canola to seed row and side banded ammonium sulfate and ammonium thiosulfate. *Journal of Agricultural Production*, *3*(1), 1–8. https://doi.org/10.29329/agripro.2022.413.1

Mitsch, W. J., Bernal, B., Nahlik, A. M., Mander, Ü., Zhang, L., Anderson, C. J., et al. (2013). Wetlands, carbon, and climate change. *Landscape Ecology*, *28*(4), 583–597. https://doi.org/10.1007/s10980-012-9758-8

Morse, J. L., & Bernhardt, E. S. (2013). Using 15N tracers to estimate N_2O and N_2 emissions from nitrification and denitrification in coastal plain wetlands under contrasting land-uses. *Soil Biology and Biochemistry*, *57*, 635–643. https://doi.org/10.1016/j.soilbio.2012.07.025

Moss, B., Kosten, S., Meerhoff, M., Battarbee, R. W., Jeppesen, E., Mazzeo, N., et al. (2011). Allied attack: Climate change and eutrophication. *Inland Waters*, *1*(2), 101–105. https://doi.org/10.5268/IW-1.2.359

Muhammad, A., Evenson, G. R., Stadnyk, T. A., Boluwade, A., Jha, S. K., & Coulibaly, P. (2018). Assessing the importance of potholes in the Canadian Prairie Region under future climate change scenarios. *Water*, *10*(11), 1657. https://doi.org/10.3390/w10111657

Neubauer, S. C., & Megonigal, J. P. (2015). Moving beyond global warming potentials to quantify the climatic role of ecosystems. *Ecosystems*, *18*(6), 1000–1013. https://doi.org/10.1007/s10021-015-9879-4

Pennock, D., Yates, T., Bedard-Haughn, A., Phipps, K., Farrell, R., & McDougal, R. (2010). Landscape controls on N_2O and CH_4 emissions from freshwater mineral soil wetlands of the Canadian Prairie Pothole region. *Geoderma*, *155*(3), 308–319. https://doi.org/10.1016/j.geoderma.2009.12.015

Petrescu, A. M. R., Lohila, A., Tuovinen, J.-P., Baldocchi, D. D., Desai, A. R., Roulet, N. T., et al. (2015). The uncertain climate footprint of wetlands under human pressure. *Proceedings of the National Academy of Sciences of the United States of America*, *112*(15), 4594–4599. https://doi.org/10.1073/pnas.1416267112

QGIS Development Team. (2020). *QGIS geographic information system* [Software]. QGIS Association.

R Core Team. (2022). *R: A language and environment for statistical computing* [Software]. R Foundation for Statistical Computing. Retrieved from https://www.R-project.org/

Rosentreter, J. A., Borges, A. V., Deemer, B. R., Holgerson, M. A., Liu, S., Song, C., et al. (2021). Half of global methane emissions come from highly variable aquatic ecosystem sources. *Nature Geoscience*, *14*(4), 225–230. https://doi.org/10.1038/s41561-021-00715-2

Segarra, K. E. A., Schubotz, F., Samarkin, V., Yoshinaga, M. Y., Hinrichs, K.-U., & Joye, S. B. (2015). High rates of anaerobic methane oxidation in freshwater wetlands reduce potential atmospheric methane emissions. *Nature Communications*, *6*(1), 7477. https://doi.org/10.1038/ncomms8477

Solomon, C., Collier, J., Berg, G., & Glibert, P. (2010). Role of urea in microbial metabolism in aquatic systems: A biochemical and molecular review. *Aquatic Microbial Ecology*, *59*, 67–88. https://doi.org/10.3354/ame01390

Soued, C., Bogard, M. J., Finlay, K., Bortolotti, L. E., Leavitt, P. R., Badiou, P., et al. (2024). Salinity causes widespread restriction of methane emissions from small inland waters. *Nature Communications*, *15*(1), 717. https://doi.org/10.1038/s41467-024-44715-3

Soued, C., del Giorgio, P. A., & Maranger, R. (2016). Nitrous oxide sinks and emissions in boreal aquatic networks in Québec. *Nature Geoscience*, *9*(2), 116–120. https://doi.org/10.1038/ngeo2611

Soued, C., & Prairie, Y. T. (2020). The carbon footprint of a Malaysian tropical reservoir: Measured versus modelled estimates highlight the underestimated key role of downstream processes. *Biogeosciences*, *17*(2), 515–527. https://doi.org/10.5194/bg-17-515-2020

Speir, S. L., Tank, J. L., Taylor, J. M., & Grose, A. L. (2023). Temperature and carbon availability interact to enhance nitrous oxide production via denitrification in alluvial plain river sediments. *Biogeochemistry*, *165*(2), 191–203. https://doi.org/10.1007/s10533-023-01074-3

Statistics Canada. (2023). Table 32-10-0038-01 Fertilizer shipments to Canadian agriculture and export markets, by product type and fertilizer year, cumulative data (x 1,000) [Dataset]. https://doi.org/10.25318/3210003801-eng

Stets, E. G., Butman, D., McDonald, C. P., Stackpoole, S. M., DeGrandpre, M. D., & Striegl, R. G. (2017). Carbonate buffering and metabolic controls on carbon dioxide in rivers. *Global Biogeochemical Cycles*, *31*(4), 663–677. https://doi.org/10.1002/2016GB005578

Tangen, B. A., & Bansal, S. (2019). Hydrologic lag effects on wetland greenhouse gas fluxes. *Atmosphere*, *10*(5), 269. https://doi.org/10.3390/atmos10050269

Tangen, B. A., & Bansal, S. (2022). Prairie wetlands as sources or sinks of nitrous oxide: Effects of land use and hydrology. *Agricultural and Forest Meteorology*, *320*, 108968. https://doi.org/10.1016/j.agrformet.2022.108968

Tranvik, L. J., Downing, J. A., Cotner, J. B., Loiselle, S. A., Striegl, R. G., Ballatore, T. J., et al. (2009). Lakes and reservoirs as regulators of carbon cycling and climate. *Limnology & Oceanography*, *54*(6), 2298–2314. https://doi.org/10.4319/lo.2009.54.6_part_2.2298

U.S. Geological Survey. (2015). Gmannppr—ScienceBase-Catalog [Dataset]. Retrieved from https://www.sciencebase.gov/catalog/item/54aeaef2e4b0cdd4a5caedf1

Vachon, D., Langenegger, T., Donis, D., Beaubien, S. E., & McGinnis, D. F. (2020). Methane emission offsets carbon dioxide uptake in a small productive lake. *Limnology and Oceanography Letters*, *5*(6), 384–392. https://doi.org/10.1002/lol2.10161

van der Kamp, G., Stolte, W. J., & Clark, R. G. (1999). Drying out of small prairie wetlands after conversion of their catchments from cultivation to permanent brome grass. *Hydrological Sciences Journal*, *44*(3), 387–397. https://doi.org/10.1080/02626669909492234

Waiser, M. J., & Robarts, R. D. (2004). Net heterotrophy in productive prairie wetlands with high DOC concentrations. *Aquatic Microbial Ecology*, *34*(3), 279–290. https://doi.org/10.3354/ame034279

Wang, X., He, Y., Yuan, X., Chen, H., Peng, C., Yue, J., et al. (2017). Greenhouse gases concentrations and fluxes from subtropical small reservoirs in relation with watershed urbanization. *Atmospheric Environment*, *154*, 225–235. https://doi.org/10.1016/j.atmosenv.2017.01.047

19449224, 2025, 3, Downloaded from https://agupubs.onlinelibrary.wiley.com/doi/10.1029/2024GB008209 by University Of Lethbridge, Wiley Online Library on [09/07/2025]. See the Terms and Conditions (https://onlinelibrary.wiley.com/terms-and-conditions) on Wiley Online Library for rules of use; OA articles are governed by the applicable Creative Commons License

Wanninkhof, R. (1992). Relationship between wind speed and gas exchange over the ocean. *Journal of Geophysical Research*, *97*(C5), 7373–7382. https://doi.org/10.1029/92JC00188

Webb, J. R., Clough, T. J., & Quayle, W. C. (2021). A review of indirect N_2O emission factors from artificial agricultural waters. *Environmental Research Letters*, *16*(4), 043005. https://doi.org/10.1088/1748-9326/abcd00

Webb, J. R., Hayes, N. M., Simpson, G. L., Leavitt, P. R., Baulch, H. M., & Finlay, K. (2019). Widespread nitrous oxide undersaturation in farm waterbodies creates an unexpected greenhouse gas sink. *Proceedings of the National Academy of Sciences of the United States of America*, *116*(20), 9814–9819. https://doi.org/10.1073/pnas.1820389116

Webb, J. R., Leavitt, P. R., Simpson, G. L., Baulch, H. M., Haig, H. A., Hodder, K. R., & Finlay, K. (2019). Regulation of carbon dioxide and methane in small agricultural reservoirs: Optimizing potential for greenhouse gas uptake. *Biogeosciences*, *16*(21), 4211–4227. https://doi.org/10.5194/bg-16-4211-2019

West, W. E., Coloso, J. J., & Jones, S. E. (2012). Effects of algal and terrestrial carbon on methane production rates and methanogen community structure in a temperate lake sediment. *Freshwater Biology*, *57*(5), 949–955. https://doi.org/10.1111/j.1365-2427.2012.02755.x

Wetzel, R. G. (2001). 12. The nitrogen cycle. In *Limnology: Lake and river ecosystems* (3rd ed.). Academic Press. Retrieved from. https://doi.org/10.1016/C2009-0-02112-6

Wickham, H., Lin Pedersen, T., & Seidel, D. (2023). Scales: Scale functions for visualization (Version 1.3.0) [Software]. Retrieved from https://scales.r-lib.org

Wu, W., Niu, X., Yan, Z., Li, S., Comer-Warner, S. A., Tian, H., et al. (2023). Agricultural ditches are hotspots of greenhouse gas emissions controlled by nutrient input. *Water Research*, *242*, 120271. https://doi.org/10.1016/j.watres.2023.120271

Yves, R. (2012). An R package for structural equation modeling. *Journal of Statistical Software*, *48*(2), 1–36. https://doi.org/10.18637/jss.v048.i02

Yvon-Durocher, G., Allen, A. P., Bastviken, D., Conrad, R., Gudasz, C., St-Pierre, A., et al. (2014). Methane fluxes show consistent temperature dependence across microbial to ecosystem scales. *Nature*, *507*(7493), 488–491. https://doi.org/10.1038/nature13164

Erratum

In the originally published version of this article, the authors used Equation 2 to calculate the gas transfer coefficient (k) of each greenhouse gas:

$$k_{\text{gas}} = k_{600}\left(\frac{Sc_{\text{gas}}}{Sc_{600}}\right)^{n} \quad (2)$$

where n is a constant that ranges from −0.67 to −0.5; however, the authors used an outdated reference (Cole & Caraco, 1998), which erroneously stated the allowed range to be −0.67 to 1. As such, the n that was chosen (+0.67) is too high and resulted in fluxes being, on average, approximately 20% higher than corrected fluxes (when using the more appropriate $n = -0.67$). This error had no impact on any trends or the conclusions. Several corrections were made to the article. The fourth sentence of the Abstract has been corrected to the following: "Wetlands in cropped landscapes had double the aquatic diffusive emissions (17.8 ± 29.3 vs. 7.7 ± 13.9 g CO_2-*eq* m^{-2} d^{-1}) … ." The eighth sentence of the Abstract has been corrected to the following: "While our estimates of aquatic CH_4 emissions from PPR wetlands were high (15.6 ± 37.2 mmol CH_4 m^{-2} d^{-1}) … ." The sentence after Equation 2 in Section 2.4 has been changed to the following: "and n is a constant that we made equal to 0.67 (but which can vary from −0.67 to −0.5; Jähne et al., 1987; Ledwell, 1984)." The second sentence of the first paragraph of Section 3.2 has been corrected to the following: "The mean fluxes of CO_2, CH_4, and N_2O were 97.3 ± 125.3, 15.6 ± 37.2, and 0.003 ± 0.016 mmol m^{-2} d^{-1}, respectively (Table S4 in Supporting Information S1)." The fourth sentence of the second paragraph of Section 3.2 has been corrected to the following: "Similarly, the across-site variability in the fluxes were 2.1 and 4.2 times higher than within-site variability for CO_2 and CH_4; the mean range in the across-site GHG fluxes was 399.1 ± 231.0 for CO_2, 170.9 ± 181.7 for CH_4, and 0.100 + 0.104 mmol m^{-2} d^{-1} for N_2O, versus within-site flux ranges of 189.3 ± 153.9 for CO_2, 40.6 ± 72.7 for CH_4, and 0.018 ± 0.039 mmol m^{-2} d^{-1} for N_2O." The fourth sentence of Section 3.3 has been corrected to the following: "While there was only a marginal difference in the flux of CO_2 and N_2O between the two land use categories (Kruskal-Wallis test: $p = 0.038$ and 0.070, respectively, Figures 4d and 4f) … ." The sixth sentence of the same paragraph has been corrected to the following: "The CH_4 flux had a mean of 23.4 ± 46.6 mmol m^{-2} d^{-1} in the cropped wetlands versus 7.7 ± 21.8 mmol m^{-2} d^{-1}… ." The first and second sentences of the first paragraph of Section 4.3 have been corrected to the following: "The rates of diffusive aquatic CH_4 emissions from wetlands in cropped landscapes reported here (mean = 23.4, range = −0.002 to 445.1 mmol m^{-2} d^{-1}) are higher than for other wetlands (Figure 8, Table S5 in Supporting Information S1). The mean diffusive aquatic CH_4 flux from wetlands in perennial landscapes in this study (mean = 7.7, range = −0.005 to 198.1 mmol m^{-2} d^{-1}) was similar to other estimates for wetlands in perennially vegetated landscapes of the PPR (Table S5 in Supporting Information S1)." The second sentence of the first paragraph of Section 4.4 has been corrected to the following: "On average, the CO_2 flux rate was positive (97.3 ± 125.34 mmol m^{-2} d^{-1}) … ." Figures 4, 5, and 7 have been replaced. The supporting information has been replaced. This may be considered the authoritative version of record.

19449224, 2025, 3, Downloaded from https://agupubs.onlinelibrary.wiley.com/doi/10.1029/2024GB008209 by University Of Lethbridge, Wiley Online Library on [09/07/2025]. See the Terms and Conditions (https://onlinelibrary.wiley.com/terms-and-conditions) on Wiley Online Library for rules of use; OA articles are governed by the applicable Creative Commons License